## Pulmonary Infection Caused by *Mycobacterium shinjukuense*

*To the Editor*:

The burden of pulmonary nontuberculous mycobacterial infection appears to be increasing worldwide. To date, more than 150 nontuberculous mycobacteria (NTM) species have been identified, and approximately 50 species have been newly described in just the last 8 years. We present a case of a patient infected with a recently discovered NTM named *Mycobacterium shinjukuense*, confirmed by 16S rRNA gene analysis of organisms recovered from bronchial lavage fluid.

### Case Summary

A 73-year-old woman was referred to our hospital because of an abnormal chest radiograph. Computed tomographic (CT) imaging of the chest showed bilateral infiltrates, many of which appeared to be centered on peripheral airways. Multiple nodules and marked bronchiectasis were found in the middle lobe and lingula (Figure 1).

Expectorated sputum revealed acid-fast bacilli (AFB). A culture of the sputum grew a nontuberculous *Mycobacterium*, which was not otherwise identified. Bronchial lavage fluid obtained from the right lower lobe also stained strongly positive for AFB. A nontuberculous *Mycobacterium* isolated from the lavage fluid could not be identified by DNA–DNA hybridization; however, analysis of the 16S rRNA gene identified the NTM as *M. shinjukuense*.

*M. shinjukuense* is a novel nonchromogenic species of NTM that was isolated from a patient in the Shinjuku Ward, a central location of Tokyo, Japan, in 2004. It was first reported by Saito and colleagues (1) in 2010. As determined by a phylogenetic analysis concatenation of the 16S rRNA gene, β-subunit of RNA polymerase, and heat-shock protein 65, *M. shinjukuense* was classified into group III of the *Runyon* classification (2), which includes *Mycobacterium tuberculosis*, *Mycobacterium ulcerans*, and *Mycobacterium marinum*; however, *M. shinjukuense* does not fall within the *M. tuberculosis* complex.

As of February 2015, 21 cases of *M. shinjukuense* lung infection have been reported, including a case report written in English (3), another case report in Japanese (4), and 19 cases reported in abstracts presented at Japanese scientific meetings. Of the 21 cases, sex and age were available in 15 and 13 cases, respectively. The ratio of male to female patients was 1:2. The median age of the 13 patients was 63 years, ranging from a patient 18 years old to patients in their 90s. Chest computed tomography imaging reportedly showed cavitary lesions in six cases, bronchiectasis in fix cases, nodules in three cases, infiltrates in two cases, ground-glass opacities in one case, and pleural thickening in one case (some patients overlapped).

In the present study, the minimum inhibitory concentrations of isoniazid, rifampicin, and ethambutol for *M. shinjukuense* isolated from our patient were ≤0.2, ≤0.03, and ≤1.0 μg/ml, respectively. Accordingly, we treated our patient with combinations of isoniazid, rifampicin, and ethambutol. Repeat chest computed tomography imaging performed 5 months after initiation of treatment showed improvement in the radiographic infiltrates. Three of four

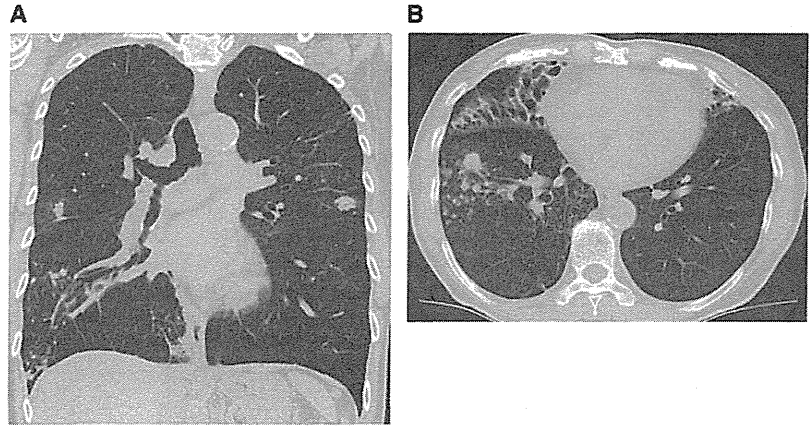


**Figure 1.** Representative coronal (*A*) and axial (*B*) chest computed tomography images showing the infection before onset of treatment.

previously reported patients who were treated with this same drug combination also responded successfully to treatment.

Aono and colleagues reported strains of AFB that were positive by TRCRapid M. TB assay (Tosoh Bioscience, Tokyo, Japan) and Amplified MTD Test (Hologic, Bedford, MA), which were subsequently identified as *M. shinjukuense* (5). Watanabe and colleagues (3) reported a case of lung infection by *M. shinjukuense* that was successfully treated with antituberculous agents. The case was initially diagnosed as pulmonary tuberculosis by sputum examination, using the TRCRapid M. TB assay. These observations suggest that the TRCRapid M. TB and Amplified MTD assays may not reliably distinguish between *M. tuberculosis* and *M. shinjukuense*. This misdiagnosis might happen because *M. shinjukuense* is most closely related to *M. tuberculosis* type strain H37Rv in a comparison of 16S rRNA gene sequences (21 base differences in 1,508 base pairs; 98.6% 16S rRNA gene sequence similarity) (1).

In cases with identification of *M. tuberculosis* infection using either TRCRapid M. TB assay or Amplified MTD Test from the samples of the patients with less risk for *M. tuberculosis* infection, such as those who are well-nourished or immunocompetent, and atypical chest images, such as remarkable bronchiectasis in the middle lobe or lingula (as in the present case), we should confirm the negative result of polymerase chain reaction of *M. tuberculosis* DNA and then consider other assays, including 16S rRNA gene analysis, for full identification.

Because only sporadic cases infected with this NTM have been reported, *M. shinjukuense* does not appear to transmit among humans similar to *M. tuberculosis*. Identification of *M. shinjukuense* from an appropriate specimen with optimal methods is critically important to avoid unnecessary infection control and relieve patients' anxiety.

**Author disclosures** are available with the text of this letter at www.atsjournals.org.

Kengo Oshima, M.D., Ph.D.
Hiroshi Yokouchi, M.D., Ph.D.
Hiroyuki Minemura, M.D.
Junpei Saito, M.D., Ph.D.
Yoshinori Tanino, M.D., Ph.D.
Mitsuru Munakata, M.D., Ph.D.
*Fukushima Medical University*
*Fukushima, Japan*

## References

1 Saito H, Iwamoto T, Ohkusu K, Otsuka Y, Akiyama Y, Sato S, Taguchi O, Sueyasu Y, Kawabe Y, Fujimoto H, *et al. Mycobacterium shinjukuense* sp. nov., a slowly growing, non-chromogenic species isolated from human clinical specimens. *Int J Syst Evol Microbiol* 2011;61:1927–1932.
2 Runyon EH. Anonymous mycobacteria in pulmonary disease. *Med Clin North Am* 1959;43:273–290.
3 Watanabe K, Shinkai M, Yamaguchi N, Shinoda M, Hara Y, Ishigatsubo Y, Kaneko T. Mycobacterium shinjukuense lung disease that was successfully treated with antituberculous drugs. *Intern Med* 2013;52: 2653–2655.
4 Futatsugi K, Nishio K, Aida S, Okabayashi K, Nakano Y, Ryuzaki M, Oosone Y, Kazumi Y. [Case report: a case of pulmonary infectious disease due to *Mycobacterium shinjukuense*]. *Nippon Naika Gakkai Zasshi* 2011;100:3637–3639. (in Japanese).
5 Aono A, Kazumi Y, Maeda S, Azuma Y, Tsuchiya S, Iwamoto T, Nakanaga K, Hayakawa K, Saito H. [Non-tuberculous mycobacterium strains that show positive test for identification kits of *M. tuberculosis* complex]. *Kekkaku* 2010;85:461–464. (Non-tuberculous mycobacterium strains that show positive test for identification kits of M. tuberculosis complex). (in Japanese).

IAI
Journals.ASM.org

# Dendritic Cell-Based Immunization Ameliorates Pulmonary Infection with Highly Virulent *Cryptococcus gattii*

**Keigo Ueno,[a] Yuki Kinjo,[a] Yoichiro Okubo,[b] Kyoko Aki,[b] Makoto Urai,[a] Yukihiro Kaneko,[a,c] Kiminori Shimizu,[d] Dan-Ni Wang,[e*] Akiko Okawara,[a] Takuya Nara,[a] Kayo Ohkouchi,[a] Yuki Mizuguchi,[a] Susumu Kawamoto,[d] Katsuhiko Kamei,[e,f] Hideaki Ohno,[a,g] Yoshihito Niki,[h] Kazutoshi Shibuya,[b] Yoshitsugu Miyazaki[a]**

Department of Chemotherapy and Mycoses, National Institute of Infectious Diseases, Tokyo, Japan[a]; Department of Surgical Pathology, Toho University School of Medicine, Tokyo, Japan[b]; Department of Bacteriology, Graduate School of Medicine, Osaka City University, Osaka, Japan[c]; Division of Molecular Biology, Medical Mycology Research Center, Chiba University, Chiba, Japan[d]; Division of Clinical Research, Medical Mycology Research Center, Chiba University, Chiba, Japan[e]; Division of Control and Treatment of Infectious Diseases, Chiba University Hospital, Chiba, Japan[f]; Department of Infectious Diseases and Infection Control, Saitama Medical Center, Saitama Medical University, Saitama, Japan[g]; Division of Clinical Infectious Diseases, Department of Internal Medicine, Showa University School of Medicine, Tokyo, Japan[h]

**Cryptococcosis due to a highly virulent fungus, *Cryptococcus gattii*, emerged as an infectious disease on Vancouver Island in Canada and surrounding areas in 1999, causing deaths among immunocompetent individuals. Previous studies indicated that *C. gattii* strain R265 isolated from the Canadian outbreak had immune avoidance or immune suppression capabilities. However, protective immunity against *C. gattii* has not been identified. In this study, we used a gain-of-function approach to investigate the protective immunity against *C. gattii* infection using a dendritic cell (DC)-based vaccine. Bone marrow-derived dendritic cells (BMDCs) efficiently engulfed acapsular *C. gattii* (Δ*cap60* strain), which resulted in their expression of costimulatory molecules and inflammatory cytokines. This was not observed for BMDCs that were cultured with encapsulated strains. When Δ*cap60* strain-pulsed BMDCs were transferred to mice prior to intratracheal R265 infection, significant amelioration of pathology, fungal burden, and the survival rate resulted compared with those in controls. Multinucleated giant cells (MGCs) that engulfed fungal cells were significantly increased in the lungs of immunized mice. Interleukin 17A (IL-17A)-, gamma interferon (IFN-γ)-, and tumor necrosis factor alpha (TNF-α)-producing lymphocytes were significantly increased in the spleens and lungs of immunized mice. The protective effect of this DC vaccine was significantly reduced in IFN-γ knockout mice. These results demonstrated that an increase in cytokine-producing lymphocytes and the development of MGCs that engulfed fungal cells were associated with the protection against pulmonary infection with highly virulent *C. gattii* and suggested that IFN-γ may have been an important mediator for this vaccine-induced protection.**

Inhalation of the airborne fungal pathogens *Cryptococcus neoformans* and *Cryptococcus gattii* causes life-threatening infectious diseases despite treatment with antifungal drugs. These two species are genetically close, although they have some distinct features. *C. neoformans* typically causes fatal infections, such as meningitis, in immunocompromised hosts, whereas *C. gattii* causes similar infections in immunocompetent hosts. Although cryptococcosis caused by *C. gattii* is endemic in tropical areas, such as Australia and Papua New Guinea, outbreaks of *C. gattii*, including fatalities among healthy individuals, were reported on Vancouver Island and surrounding areas beginning in 1999 (1, 2). In response to this, the Centers for Disease Control and Prevention (CDC) of the United States and British Columbia organized a public health working group to promote awareness of this outbreak (3–5).

Using mouse pulmonary infection models, two groups independently showed that *C. gattii* strain R265, which was clinically isolated during the Canadian outbreak, was more virulent than *C. neoformans* strain H99, which is frequently studied (6, 7). Although the mechanisms for its hypervirulence remain unknown, there is evidence that *C. gattii* induces a less severe inflammatory response than that induced by *C. neoformans* infection. Histological and flow cytometry analyses showed reduced migration of inflammatory cells into the lungs of mice infected with R265 compared with those infected with H99 (7–9). Additionally, a smaller amount of inflammatory cytokines was found in the lungs of mice infected with *C. gattii* (9) and in the cerebrospinal fluid of humans infected with *C. gattii* (10, 11). These findings suggest that *C. gattii* has a superior ability to suppress or evade the inflammatory response.

Previous studies indicated that one of the capsular components of *C. gattii* may have been involved in immune avoidance or immune suppression and was required for the complete virulence of *C. gattii* (12, 13). Because *C. gattii* can induce immune avoidance or suppression, an analysis of loss-of-function using gene knockout (KO) mice is not applicable for studying any protective immune responses against *C. gattii*, and the protective immunity

Received 30 December 2014 Returned for modification 19 January 2015
Accepted 27 January 2015
Accepted manuscript posted online 2 February 2015
Citation Ueno K, Kinjo Y, Okubo Y, Aki K, Urai M, Kaneko Y, Shimizu K, Wang D-N, Okawara A, Nara T, Ohkouchi K, Mizuguchi Y, Kawamoto S, Kamei K, Ohno H, Niki Y, Shibuya K, Miyazaki Y. 2015. Dendritic cell-based immunization ameliorates pulmonary infection with highly virulent *Cryptococcus gattii*. Infect Immun 83:1577–1586. doi:10.1128/IAI.02827-14.
Editor: G. S. Deepe, Jr.
Address correspondence to Yuki Kinjo, ykinjo@niid.go.jp.
* Present address: Dan-Ni Wang, Department of Medical Microbiology and Parasitology, School of Medicine, Shanghai Jiao Tong University, Shanghai, China.
Supplemental material for this article may be found at http://dx.doi.org/10.1128/IAI.02827-14.

doi:10.1128/IAI.02827-14

against highly virulent *C. gattii* has not been well characterized. Thus, it is important to unravel any protective immunity against *C. gattii* to garner insights for the prevention, diagnosis, and treatment of cryptococcosis with highly virulent *C. gattii*.

Dendritic cells (DCs) play a central role in inducing effector T cells (14) and can also be utilized as antigen delivery systems for vaccinations for cancers or infections (15, 16). Adoptive transfer of DCs pulsed with fungal cells or with fungal RNA has also been utilized as a means to assess T cell-mediated immunity against pathogenic fungi (17–19). In this study, we implemented a gain-of-function approach to investigate protective immunity against *C. gattii*. We tested whether a DC-based vaccine could augment protective immunity against the highly virulent *C. gattii* strain R265 by evaluating the pathology, fungal burden, and survival rate after pulmonary infection in mice. Further, we examined cytokine-producing cells in the mouse spleen and lung. Moreover, we assessed the role of gamma interferon (IFN-γ) in the protective effect exerted by this DC-based vaccine using IFN-γ knockout mice.

## MATERIALS AND METHODS

**Ethics.** All our animal experiments were in compliance with the guidelines and policies of the Principles of Morality for Animal Experiments of the National Institute of Infectious Disease, Japan (approval numbers 213072, 21608, 214044, 114004, and 114029).

**Mice.** C57BL/6J mice were purchased from Japan SLC, Inc. IFN-γ knockout (KO) mice (C57BL/6 background) were purchased from the Jackson Laboratory. Mice used in experiments were 6 to 8 weeks old and were maintained under specific-pathogen-free conditions at the National Institute of Infectious Diseases of Japan.

***C. gattii.*** *C. gattii* strain R265 (genotype VGII, mating type α, and serotype B) was kindly provided by Kyung J. Kwon-Chung (National Institutes of Health, Bethesda, MD); in 2001, this strain was clinically isolated from bronchial washings of infected patients during the Vancouver Island outbreak (20). To construct the acapsular *C. gattii* Δ*cap60* strain, *CAP60* (GenBank accession number CGB_A6290C) of *C. gattii* strain PNG18 (genotype VGI, mating type α, and serotype B) was disrupted by gene replacement using the nourseothricin resistance gene *NAT1*, which was also clinically isolated from an infected person in Papua New Guinea (21). The disruption strategy used is shown in Fig. S1 in the supplemental material. The primers and sequences that were used for strain construction are listed in Table S1 in the supplemental material.

To prepare a gene replacement cassette, DNA fragments, such as for a marker gene and homologous regions, were amplified by PCR. The marker fragment *NAT*, including the *ACT1* promoter, *NAT1*, and the *TRP1* terminator, were amplified using the primers NAT-F and NAT-R derived from plasmid pCH233 used as a template (22). Homologous upstream and downstream regions (≈1 kb) of *CAP60* were amplified with the primers CAP60up-F and CAP60up-R for the upstream region and CAP60down-F and CAP60down-R for the downstream region using *C. gattii* genomic DNA as a template. The primer pairs CAP60up-R and NAT-R and CAP60down-F and NAT-F contained complementary sequences that allowed them to anneal with the marker fragment *NAT*. Three fragments, (i) 5′ upstream region, (ii) 3′ downstream region, and (iii) *NAT* fragment, were equally mixed and used as a template for PCR with the primers CAP60up-F and CAP60down-R, which harbored a single gene disruption cassette. This cassette was introduced into *C. gattii* strain PNG18 using a helium-driven biolistic system (Bio-Rad) as described previously (23). The transformants were screened on a yeast extract-peptone-dextrose (YPD) agar plate (1% [wt/vol] yeast extract, 2% [wt/vol] Bacto peptone, and 2% [wt/vol] dextrose) that contained 100 μg/ml of nourseothricin. Homologous integration events were confirmed by PCR using the primers shown in Fig. S1. The *CAP60* open reading frame (ORF), the region from the ATG codon to the TAG stop codon, was completely deleted in the Δ*cap60* strain.

Plasmid pJAF12-CAP60 was constructed to integrate the *CAP60* ORF with a 1-kb flanking region into the genomic DNA of the Δ*cap60* strain. Primers CAP60up-NotI-F and CAP60down-SacII-R were used to amplify the *CAP60* locus, and the amplified fragment was digested with NotI and SacII. The digested fragment was cloned into the NotI and SacII sites of pJAF12 (24). Plasmid pJAF12-CAP60 was introduced in the Δ*cap60* strain as described above, and the transformants were screened on a YPD agar plate that contained 100 μg/ml of nourseothricin and 200 μg/ml of Geneticin (G418). Homologous integration events were confirmed by PCR with the primers shown in Fig. S1 in the supplemental material.

To prepare heat-killed fungal cells, *C. gattii* was cultured in YPD medium with shaking overnight at 30°C. Cells were harvested and washed with sterile Dulbecco's phosphate-buffered saline (DPBS; Invitrogen), resuspended in DPBS, and boiled for 1 h. Heat-killed *C. gattii* cells were not washed further. The morphologies of heat-killed *C. gattii* were not altered based on microscopic observations. A suspension of heat-killed *C. gattii* cells was spread onto YPD agar and cultured at 30°C for 7 days to check whether all *C. gattii* cells were dead.

A conventional India ink preparation was used to observe capsule formation. *C. gattii* cells were grown in YPD medium at 30°C with shaking overnight. Then, 100 μl of a culture suspension was centrifuged and the harvested cells were resuspended in 20 μl of an ink solution, which included equal amounts of 4% (wt/vol) paraformaldehyde and India ink. Then, 5 μl of an ink-cell suspension was placed on a slide glass with a coverslip. Cells were observed by differential interference contrast microscopy (Inverted microscope IX81; Olympus).

**BMDCs.** Bone marrow (BM) cells were harvested from the femurs and tibias of female C57BL/6J mice. Red blood cells were lysed with lysis buffer (9 volumes of 0.83% [wt/vol] $NH_4Cl$ and 1 volume of 200 mM Tris-HCl, pH 7.6). BM cells ($3 \times 10^6$ cells/10 ml per dish) were cultured in RPMI 1640 (complete) medium (Sigma) supplemented with 10% (vol/vol) fetal bovine serum (FBS), 1% (vol/vol) streptomycin-penicillin solution (Sigma; 10,000 U of penicillin and 10 mg/ml of streptomycin), 44 μM 2-mercaptoethanol, and 10 ng/ml of mouse granulocyte-macrophage colony-stimulating factor (mGM-CSF; PeproTech, Inc.) at 37°C under 5% $CO_2$. Sterile petri dishes (not treated for cell culture) were used for cell culture. On day 3, 6 ml of the culture medium was removed, and 7 ml of fresh complete medium was added to the dishes. On day 5, 5 ml of fresh complete medium was added to the dishes. On day 6, nonadherent cells were collected and used as BM-derived dendritic cells (BMDCs).

**Lung leukocytes.** Mouse lungs were perfused and rinsed with saline prior to being minced with scissors. Lung pieces were enzymatically digested at 37°C for 60 min with 5 ml/lung of a digestion solution (RPMI 1640 medium, 5% FBS, 2 mg/ml of collagenase D [Roche], and 10 μg/ml of DNase I [Sigma]) in 15-ml conical tubes and a tube rotator. After digestion, 250 μl of 100 mM EDTA solution was added to the tubes to stop digestion (final concentration, 5 mM EDTA). The lung pieces were then homogenized with a 70-μm cell strainer (BD-Falcon), and cell suspensions were harvested. A cell pellet was resuspended in 2 ml of 30% Percoll (GE Healthcare) and layered onto 4 ml of 44% and 70% Percoll. All Percoll solutions contained 2 mM EDTA to prevent cell aggregation. After centrifugation at 1,000 × *g* without acceleration and deceleration for 20 min at room temperature, cells at the 44-70% interface were collected and washed twice with complete RPMI 1640 medium. Cells ($2 \times 10^5$) were attached to a glass slide using a Cytofuge-12 (Statspin, Inc.) and stained with Diff-Quik (Sysmex Corporation) for Wright-Giemsa staining, followed by determination of the proportion of each cell type under a microscope. The numbers of lymphocytes, macrophages, and polymorphonuclear cells (PMNs) were determined by multiplying the total leukocyte count by the proportion of each cell type.

**Phagocytosis assay.** Prior to doing a phagocytosis assay, heat-killed *C. gattii* cells ($1 \times 10^9$ cells/ml) were stained with acridine orange (stock concentration, 0.1 mg/ml; working concentration, 0.01 mg/ml) at room

temperature for 1 h in the dark. Stained cells were washed with DPBS and resuspended in RPMI 1640 medium supplemented with 10% (vol/vol) heat-inactivated FBS. We confirmed that capsular strains as well as the wild-type strain were stained. A suspension of stained cells was stored at 4°C overnight. Harvested BMDCs ($1 \times 10^6$ cells/ml) were incubated with prestained *C. gattii* cells ($5 \times 10^6$ cells/ml; multiplicity of infection [MOI] = 5) in complete RPMI 1640 medium that contained mGM-CSF in 24-well culture plates. After incubation, 500 μl of 4% (vol/vol) paraformaldehyde (Fixation Buffer; Biolegend) was added and cells were fixed at room temperature for 5 min, followed by a washing with DPBS. Fungal cells that were not engulfed by BMDCs were stained with calcofluor white (Sigma; 1/10 dilution) at room temperature for 5 min. Culture wells were rinsed with DPBS before fluorescence microscopic analysis (inverted microscope IX81; Olympus). A mercury apo lamp, Olympus filter cube WU (BP330–385, DM400, BA420), and Olympus filter cube GFP (BP460–480, DM485, BA495–540) were used for the fluorescence imaging. At least five fields of view with ≈100 BMDCs/field were randomly selected. At least three fields were used to determine a phagocytosis rate, defined as the number of BMDCs engulfing fungal cells/total BMDCs × 100%. ImageJ software (National Institutes of Health, USA) was used for cell counting and color image merging.

**Activation marker expression on BMDCs and cytokine-producing T cells.** BMDCs ($2 \times 10^6$ cells/ml) were incubated in complete RPMI 1640 medium that contained mGM-CSF and heat-killed *C. gattii* cells ($2 \times 10^4$ cells/ml; MOI = 0.1) or 100 ng/ml of lipopolysaccharide (LPS) from *Escherichia coli* O111:B4 (Sigma) for 24 h. Cells were then collected and stained for flow cytometry analysis. All antibodies and buffer used for cell staining were from Biolegend. Fc receptors were blocked with an anti-CD16/32 antibody (clone 93), after which cells were stained with the following antibodies: anti-CD11b (clone M1/70), anti-CD11c (clone N418), anti-CD86 (clone GL-1), anti-CD40 (clone MR1), and anti-I-Ab (clone AF6-120.1).

To assess cytokine-producing T cells, spleen cells ($2 \times 10^6$ cells/ml) were cultured in complete RPMI 1640 medium with 100 ng/ml of anti-CD28 monoclonal antibody (MAb) (clone 37.51) and 100 ng/ml of anti-CD49d MAb (clone 9C10) in the presence of heat-killed Δ*cap60* cells (MOI = 0.1) for 5 to 6 days. Lung leukocytes were incubated in complete RPMI 1640 medium with 50 ng/ml of phorbol 12-myristate 13-acetate (PMA) and 1 μM ionomycin for 3 h. To stop cytokine release, brefeldin A (final concentration, 5 μg/ml; Biolegend) and monensin (final concentration, 2 μM; Sigma; stock concentration, 72 mM in methanol) were added for the last 1.5 to 4 h of culture. After blocking of Fc receptors, cell surface molecules on harvested cells were stained with the following antibodies: anti-CD4 (clone GK1.5), anti-CD3 (clone 145-2C11), and anti-Thy1.2 (clone 30-H12). Intracellular cytokines were stained according to the manufacturer's instructions (Biolegend) with the following antibodies: anti-IFN-γ (clone XMG1.2), anti-interleukin 17A (anti-IL-17A) (clone TC11-18H10.1), and anti-tumor necrosis factor alpha (anti-TNF-α) (clone MP6-XT22). For RORγt staining, a FOXP3/transcription factor staining buffer set and anti-human/mouse RORγt (clone AFKJS-9) were used according to the manufacturer's instructions (eBioscience Inc.). Isotype-matched IgG was used for control staining for IFN-γ, IL-17A, TNF-α, and RORγt. Data were acquired with a BD FACSCaliburor BD FACSCantoII flow cytometer (BD Bioscience) and analyzed using FlowJo software (TreeStar Inc.).

**Cytokine determinations.** BMDCs ($1 \times 10^6$ cells/ml) were incubated with heat-killed *C. gattii* cells for 24 h. After centrifugation, culture supernatants were collected and cytokine levels were determined by enzyme-linked immunosorbent assay (ELISA). Cytokines in lung homogenates prepared from *C. gattii*-infected mice were also measured by ELISA. A MaxiSorp plate and a DuoSet ELISA kit (R&D Systems) or BD OptEIA ELISA sets (BD Bioscience) were used according to the manufacturers' instructions.

**Vaccination.** BMDCs ($1 \times 10^6$ cells/ml) were incubated in complete RPMI 1640 medium that contained mGM-CSF and heat-killed *C. gattii* cells ($1 \times 10^7$ cells/ml; MOI = 10) for 24 h in petri dishes. After incubation, nonadherent cells were collected and washed twice with PBS. BMDCs that were pulsed with heat-killed *C. gattii* cells ($5 \times 10^5$ cells/mouse) were injected via a tail vein, both at 14 days and 1 day before intratracheal infection with *C. gattii* R265.

**Infection study.** *C. gattii* R265 was cultured in YPD at 30°C with shaking overnight. Cells were then washed and resuspended in PBS. A mouse was anesthetized with isoflurane, after which 50 μl of a fungal suspension ($3 \times 10^3$ CFU) was intratracheally injected using a 24-gauge indwelling needle (TOP Corporation, Japan). Mice were euthanized by carbon dioxide inhalation, and their lungs were harvested to determine their weight and fungal burden. Lungs were homogenized using a stainless steel mesh in 5 ml of PBS. Homogenates were diluted and spread onto YPD plates. These plates were incubated at 30°C for 24 h, after which colonies were counted.

**Histological analysis.** Histological analyses were as previously described (8). To prepare specimens, three isolated lungs were fixed in 10% formalin, dehydrated, and embedded in paraffin. Paraffin blocks were cut into 4-μm sections and stained with hematoxylin and eosin, alcian blue, or Elastica van Gieson stain for light microscopy analysis. The cross point intervals of alveoli were measured to assess alveolar spaces and the levels of alveolar destruction as described previously (25). Multinucleated giant cells (MGCs) were examined to assess macrophage recruitment into lungs after infection. The numbers of MGCs per unit area (square millimeters), the numbers of nuclei within each MGC, and the nuclear density in MGCs were determined as described previously (26).

**Statistical analysis.** GraphPad Prism5 (GraphPad Software, Inc.) was used for statistical analyses. *P* values of $<0.05$ were considered significant.

## RESULTS

**BMDCs are activated by acapsular *C. gattii*.** To design an effective DC-based vaccine, we first evaluated the phagocytosis efficiency, costimulatory molecule expression, and cytokine production by BMDCs that were cultured with *C. gattii* cells. Because the capsular component of *C. neoformans* is known to suppress several immune responses by BMDCs (27, 28), we constructed an acapsular Δ*cap60* strain (see Fig. S1 in the supplemental material) and compared this with encapsulated strains (Fig. 1). In a phagocytosis assay, 80% of BMDCs engulfed several Δ*cap60* cells within 24 h, while only 10% of BMDCs engulfed one or two cells of the encapsulated strains (Fig. 1B; see also Fig. S2 in the supplemental material). Major histocompatibility complex class II (MHC-II) molecules (I-Ab) are essential for antigen presentation to CD4 T cells, and CD86 and CD40 are important costimulatory molecules for T cell stimulation. The percentages of BMDCs that expressed these molecules were significantly increased when these cells were stimulated with the acapsular Δ*cap60* strain (Fig. 1C; see also Fig. S3 in the supplemental material). Additionally, BMDCs that were stimulated with the Δ*cap60* strain produced more inflammatory cytokines, including IL-12p40 and TNF-α, than BMDCs that were stimulated with encapsulated strains (Fig. 1D). These data showed that BMDCs could be activated by the acapsular Δ*cap60* strain and suggested that BMDCs pulsed with this strain could be used for a DC-based vaccine to induce T cell responses against *C. gattii*.

**Transferring CAP60Δ/DCs ameliorates pulmonary infection with highly virulent *C. gattii*.** We tested for a protective effect after vaccination with Δ*cap60* strain-pulsed DCs (CAP60Δ/DCs) in a mouse model of pulmonary *C. gattii* infection. Transferring CAP60Δ/DCs significantly suppressed fungal growth in mouse lungs and improved mouse survival rates after pulmonary infection with the highly virulent strain R265 (Fig. 2). Although *C.*

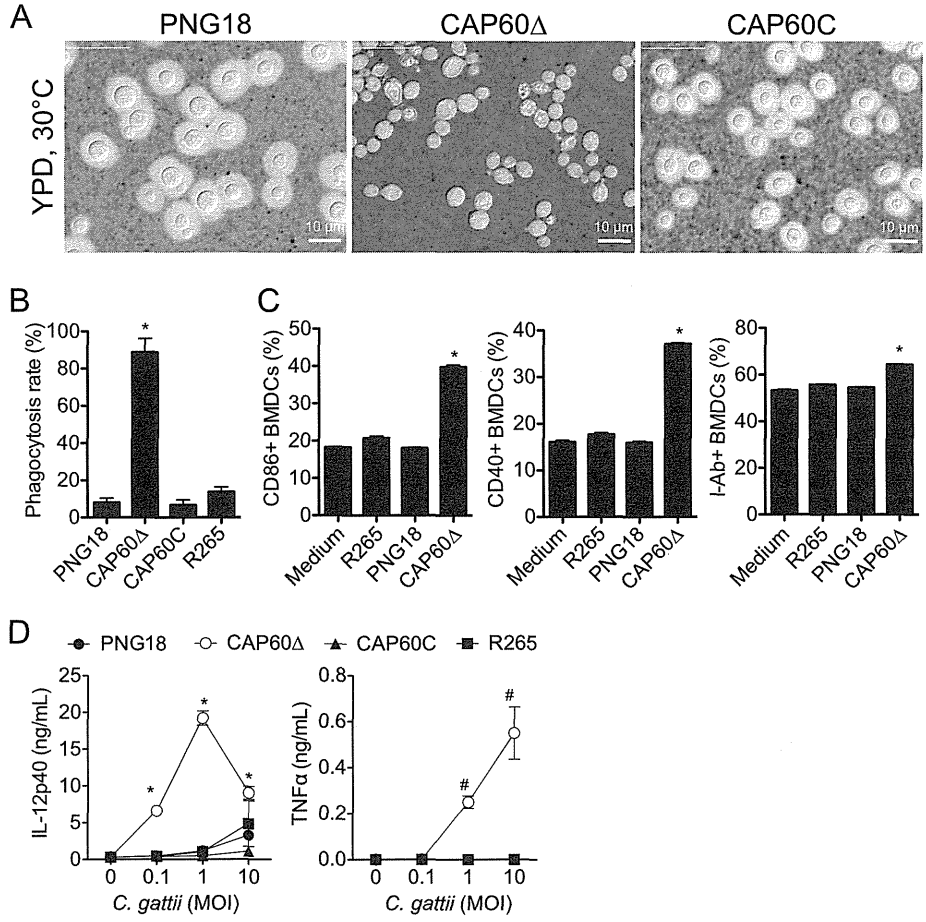


FIG 1 The *C. gattii* acapsular Δ*cap60* strain efficiently activates BMDCs. (A) Capsule formation was assessed using the conventional India ink method. Parental strain PNG18, the Δ*cap60* strain, and the revertant (CAP60C) were grown in YPD medium at 30°C overnight. BMDCs were incubated with heat-killed *C. gattii* cells for 24 h, and the phagocytosis rate (B), costimulatory molecule expression (C), and cytokine production (D) were evaluated by fluorescence microscopy, flow cytometry, and ELISA, respectively. For flow cytometry analysis, gates were set for $CD11c^+$ $CD11b^+$ cells. Representative data (means ± SDs) from 2 or 3 independent experiments are shown. *, $P < 0.05$ versus PNG18 by unpaired *t* test; #, $P < 0.05$ versus PNG18 by Mann-Whitney U test.

*neoformans* acapsular mutants have been successfully used as vaccines (29), vaccination using heat-killed R265 or heat-killed Δ*cap60* strain without DCs had no protective effect (see Fig. S4 in the supplemental material). In these experiments, we could not evaluate fungal burdens in the brain or spleen because of the limited number of fungal cells that had disseminated to the brain and spleen (data not shown). A previous study also showed that *C. gattii* R265 only minimally disseminated from the lungs to other organs in a murine pulmonary infection model (7).

To determine how our CAP60Δ/DC vaccine suppressed fungal growth, we histologically assessed mouse lung sections after pulmonary infection with highly virulent *C. gattii*. Lungs were significantly lighter in those mice immunized with our CAP60Δ/DC vaccine than in unvaccinated mice at day 13 postinfection (see Fig. S5 in the supplemental material). In unvaccinated mice, the increased numbers of fungal cells destroyed alveolar structures by enlarging alveolar spaces. In contrast, fewer fungal cells, increased numbers of leukocytes, and reduced alveolar destruction were observed in the lungs of mice that had been immunized with Δ*cap60* strain-loaded DCs (Fig. 3; see also Fig. S5 and Table S2 in the supplemental material). The majority of these leukocytes were mononuclear cells, including lymphocytes and macrophages, which developed into multinucleated giant cells (MGCs) that engulfed the fungal cells in the lungs of mice immunized with our CAP60Δ/DC vaccine. Large MGCs with a number of nuclei and an eosinophilic cytoplasm that represented the accumulated macrophages and well-matured cytoplasmic organelles, respectively, were significantly increased in immunized mice (Fig. 3C). Although transferring antigen-unloaded DCs also induced leukocyte accumulation and the development of MGCs in the lungs to some extent, MGCs with lesser eosinophilic cytoplasm and engulfing fewer fungal cells were observed in those mice that received antigen-unloaded DCs compared with those in immunized mice (Fig. 3). Increased numbers of leukocytes and multinucleated cells were also observed in the lungs of vaccinated mice at day 7 posttransfer (see Fig. S5). Taken together, these data suggested that the development of MGCs that engulfed fungal cells had suppressed the fungal growth in the lungs of immunized mice.

**Transferring CAP60Δ/DCs induces cytokine-producing lymphocytes in spleen and lungs.** The development of MGCs that

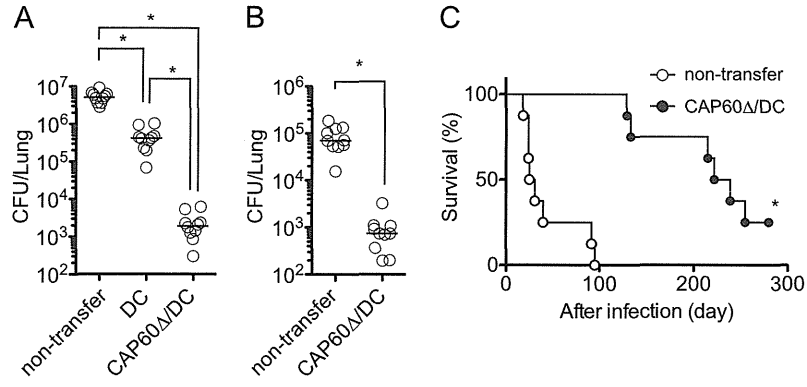


FIG 2 Transferring CAP60Δ/DCs ameliorates pulmonary infection with highly virulent *C. gattii* strain R265. CAP60Δ/DCs or unloaded DCs were injected into tail veins of mice at 14 days and 1 day prior to intratracheal infection with $3 \times 10^3$ CFU of strain R265. (A and B) Fungal burdens ($n = 5$) in the lungs were determined at day 14 (A) and day 3 (B). Pooled data from two independent experiments are plotted, and median values are shown by short horizontal lines. *, $P < 0.05$ by analysis of variance with Dunn's *post hoc* test (A) or $P < 0.05$ by Mann-Whitney U test (B). (C) Survival curves ($n = 8$) were compared by log rank test. Representative data from two independent experiments are shown. *, $P < 0.01$. Median survival times were 28 days in the case of nontransfer and 238 days in the case of CAP60Δ/DC transfer.

engulf fungal cells in granulomas is associated with protection from cryptococcosis due to *C. neoformans*, which is also associated with an increase in cytokine-producing T cells, such as Th1 and Th17 cells (30–33). Because DC-based vaccines reportedly augmented cytokine-producing effector T cells (17, 34), we assessed cytokine-producing T cells in the spleen and lungs after vaccination. IFN-$\gamma^+$ and TNF-$\alpha^+$ CD4 T cells that responded to antigen restimulation were significantly increased in the spleens of vaccinated mice at day 14 after infection (Fig. 4). However, we could not detect any IL-17A-producing T cells (data not shown). Because the numbers of total splenocytes and proportions of $CD4^+$ cells among splenocytes were equal between unvaccinated and vaccinated mice at day 14 postinfection, the increased proportion of these cells indicated an increase in the numbers of this cell population.

Also, we utilized short-pulse stimulation using phorbol 12-myristate 13-acetate (PMA) and ionomycin to determine the numbers of cytokine-producing T cells in the lungs of vaccinated mice. IL-$17A^+$ ROR$\gamma t^+$ T cells and innate lymphoid cells (ILCs) were significantly increased in the lungs of vaccinated mice at day 1 postinfection (Fig. 5). CD4 T cells that produced IL-17A, IFN-$\gamma$, or TNF-$\alpha$ were also increased in the lungs of vaccinated mice at day 7 after transfer of CAP60Δ/DCs (see Fig. S6 in the supplemental material). At day 14 after infection, the amounts of IFN-$\gamma$, IL-17A, TNF-$\alpha$, and CXCL1 (KC) were significantly increased in the lungs of immunized mice, and comparable amounts of IL-1$\beta$ and smaller amounts of CCL2 (MCP-1) were detected (see Fig. S6). Because numerous lymphocytes and macrophages had already accumulated in the lungs of immunized mice, the amounts of MCP-1 may have decreased by day 14 after infection. These data suggested that increased T cell cytokine responses in vaccinated mice may have contributed to the development of MGCs that engulfed fungal cells after pulmonary infection with *C. gattii*.

**IFN-$\gamma$ may be an important mediator for vaccine-induced protection against pulmonary infection with highly virulent *C. gattii*.** Previous studies showed that IFN-$\gamma$-producing T cells had a protective role in pulmonary infection with *C. neoformans* (35, 36). However, surprisingly, the fungal burden was significantly reduced in the lungs of IFN-$\gamma$ knockout (KO) mice after the pulmonary infection with *C. gattii* compared with that in C57BL/6J wild-type (WT) mice (Fig. 6). Thus, we investigated a role for IFN-$\gamma$ in DC vaccine-induced protection by determining the reduction rate of the fungal burden in the lungs of vaccinated mice. The DC-based vaccine induced an 8,900-fold reduction and a 2,700-fold reduction in the fungal burdens in the lungs of WT mice and IFN-$\gamma$ KO mice, respectively. The protective effect of our DC vaccine was significantly reduced in IFN-$\gamma$ knockout mice. This suggested that IFN-$\gamma$ may be an important mediator for DC vaccine-induced protection against pulmonary infection with highly virulent *C. gattii*.

## DISCUSSION

In this study, we developed a new DC-based vaccine to investigate protective immunity against highly virulent *C. gattii*. Our results showed that an increase in cytokine-producing CD4 T cells and the development of MGCs that engulfed fungal cells were associated with protection against pulmonary infection with highly virulent *C. gattii*.

Recently, Chaturvedi et al. reported a protein-based vaccine against highly virulent *C. gattii*. They identified several protein antigen candidates using two-dimensional PAGE (2D-PAGE) and immunoblotting with sera from vaccinated mice after infection (37). They immunized mice three times at 4-week intervals without any adjuvant and then challenged mice intranasally with $1 \times 10^4$ CFU of *C. gattii* R265 at 10 days after the final immunization. Although the protein vaccine significantly ameliorated the fungal burden in lungs and improved the survival rate after this challenge, this protein-based vaccine induced no more than about a 5-fold reduction in the fungal burden in lungs on day 14 postinfection (37). In our study, Δ*cap60* strain-loaded DCs were transferred at day 14 and day 1 prior to infection, and this DC-based vaccine provided for an 8,900-fold reduction in the fungal burden in mouse lungs at day 14 postinfection (Fig. 6). This DC-based vaccine still effectively suppressed fungal growth even when mice were infected with *C. gattii* at 2 months after the final transfer of CAP60Δ/DCs (unpublished data). Interestingly, vaccination with DCs loaded with the Δ*cap60* strain (VGI) effectively suppressed the growth of R265 (VGII). Thus, our data suggested that our

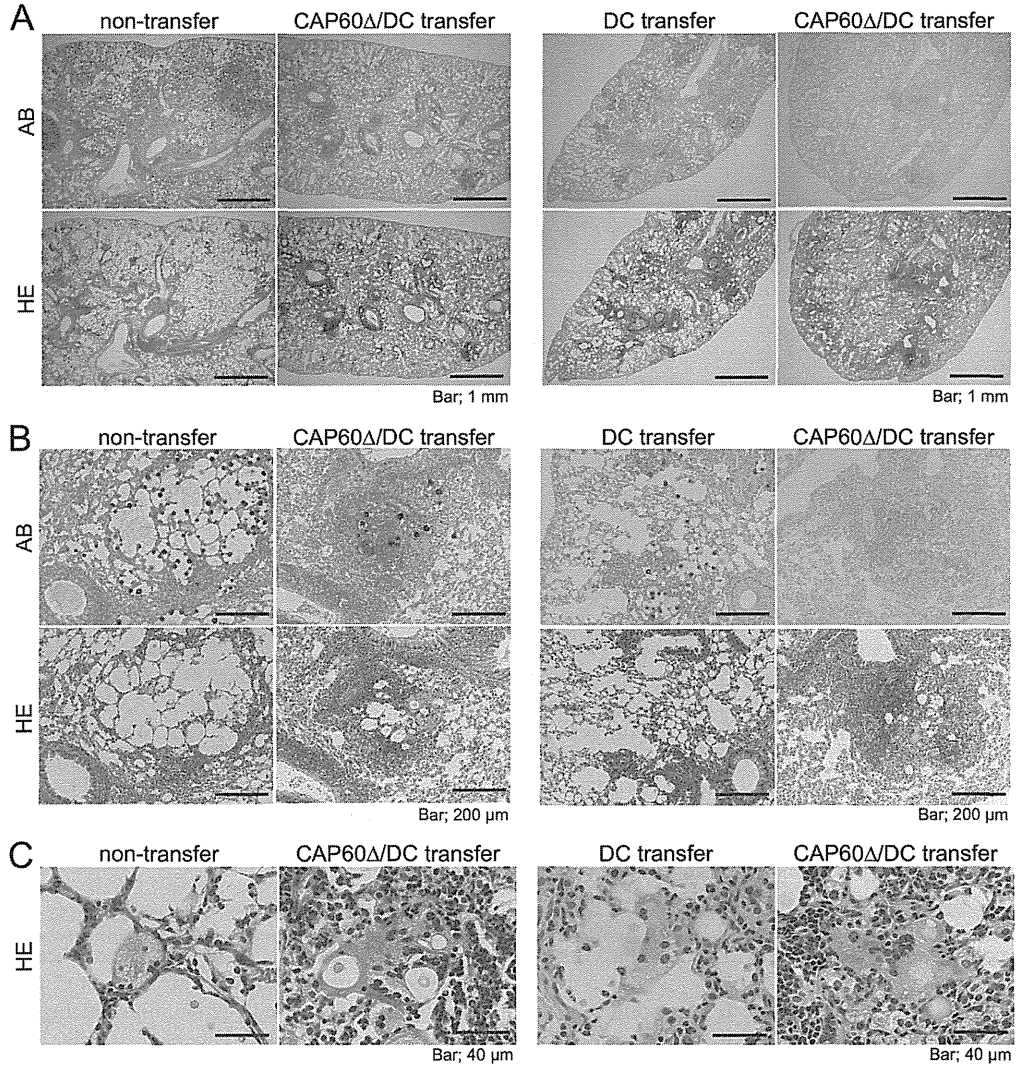


**FIG 3** Multinucleated giant cells (MGCs) engulf fungal cells in the lungs of immunized mice. Lung sections obtained from three mice, at 13 days after infection with strain R265, were stained with hematoxylin-eosin (HE) or alcian blue (AB). *C. gattii* cells were stained with alcian blue. Each section was observed at magnifications of ×40 (A), ×200 (B), and ×1,000 (C).

CAP60Δ/DC vaccine could induce protection against *C. gattii* in a cross-strain manner and that this DC-based vaccine was useful for studying protective immunity against highly virulent *C. gattii*.

Huston et al. showed that human DCs derived from $CD14^+$ peripheral blood mononuclear cells (PBMCs) could engulf and kill *C. gattii* strain R265 but that DCs failed to mature in the presence of *C. gattii* (38). They also showed that TNF-α could restore DC maturation to induce T cell responses in the presence of *C. gattii*, which suggested the potential of DC-based therapies to improve the outcomes of patients with *C. gattii* infections. Another study showed that encapsulated *C. neoformans* strain B3501 (serotype D) could induce human DC maturation based on DC expression of CD40, CD86, and MHC-II (28). In our study, murine BMDCs did not mature in the presence of encapsulated *C. gattii* strains, because they did not efficiently engulf encapsulated *C. gattii* strains (Fig. 1). One study showed that murine BMDCs could mature after upregulated CD86 and MHC-II expression and cytokine production in the presence of encapsulated *C. neoformans* strain 1841 (serotype D) (27). Thus, both human DCs and murine BMDCs can become mature in the presence of encapsulated *C. neoformans*, but they did not mature in the presence of encapsulated *C. gattii*, as the phagocytosis rate for *C. gattii* cells seemed to be different between human DCs and murine BMDCs.

This failure of DC maturation may have negatively affected protection against pulmonary infection with *C. gattii*. In fact, transferring antigen-unloaded DCs prior to infection induced about a 10-fold reduction in the fungal burden in the lungs at day 14 postinfection (Fig. 2). Because BMDCs were cultured in the presence of GM-CSF, even antigen-unloaded DCs secreted a small amount (~300 pg/ml) of IL-12p40 (Fig. 1). Thus, transferring unloaded DCs seemed to induce a small number of IFN-γ-producing CD4 T cells in the spleen (Fig. 4). However, the protective

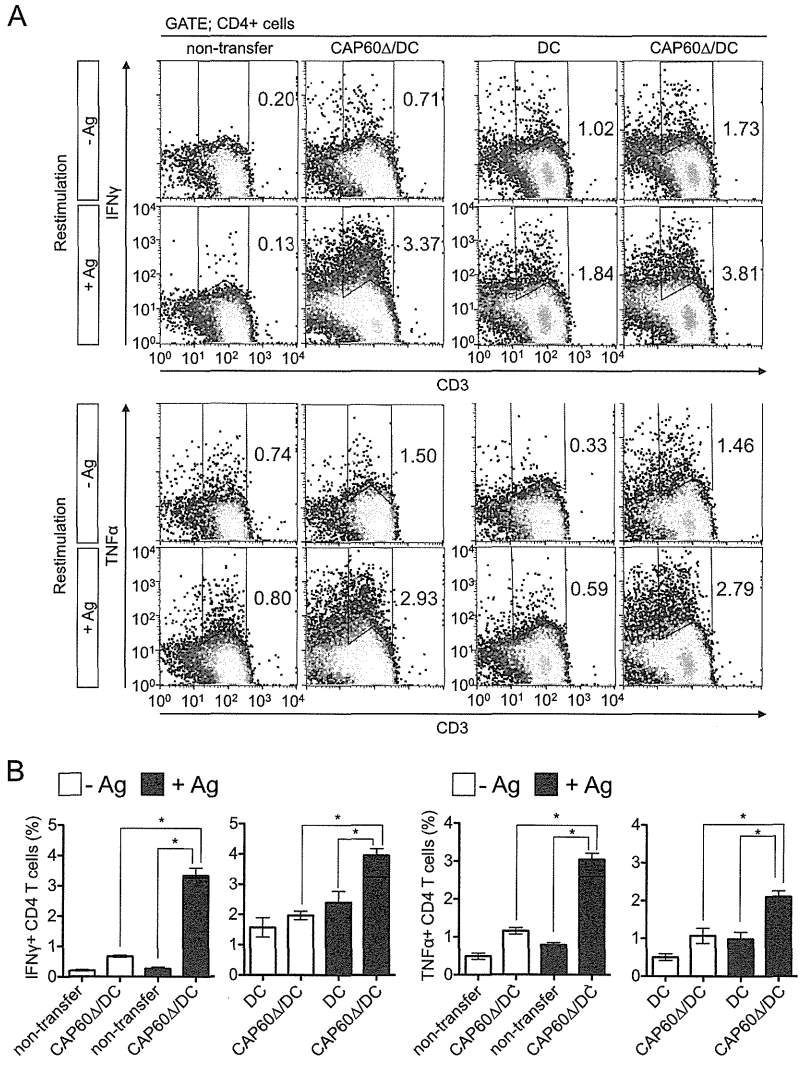


**FIG 4** Transferring CAP60Δ/DCs induces cytokine-producing CD4 T cells in spleen. Splenocytes were obtained from three mice at 14 days after infection and cultured with (+Ag) or without (−Ag) antigen and with or without heat-killed Δ*cap60* cells (MOI = 0.1) for 5 to 6 days. For flow cytometry analysis, gates were set for $CD4^+$ cells. Representative flow cytometry profiles (A) and histograms for statistical analysis (B) are shown. Pooled data from two separate experiments were used to prepare histograms (means ± SEMs). *, $P < 0.05$ by analysis of variance with Dunnett's *post hoc* test.

effect was limited in those mice that received unloaded DCs compared with the effect in those that received Δ*cap60* strain-pulsed DCs, as transferring unloaded DCs induced fewer antigen-specific T cells. These findings suggested that the complete activation of DC and T cell responses was required for protection against pulmonary infection with highly virulent *C. gattii*.

In a strict sense, vaccination using CAP60Δ/DCs only delayed the progression of infection, as the fungal burden in the lungs at day 14 after infection was not lower than the inoculated burden (Fig. 2). In fact, even though mice were immunized with CAP60Δ/DCs, most of these mice ultimately died (Fig. 2C). This implied that highly virulent *C. gattii* could cause a persistent infection or could change to a latent state during a protective immune response. Persistent infection with *C. neoformans* was shown in a previous report, as *C. neoformans* could be detected in the lungs of immunocompetent rats at 18 months after an intratracheal infection, along with reduced nitric oxide synthase in pulmonary granulomas that harbored this pathogen (39). *C. gattii* may also cause a persistent infection by similar mechanisms. To overcome persistent *C. gattii* infection, the DC-based vaccine used in this study needs to be refined. Previous studies showed that treating antigen-loaded DCs with rapamycin, an mTOR inhibitor, enhanced T cell responses and augmented the vaccine's efficacy against tuberculosis or tumors. Because rapamycin can enhance DC autophagy, which can enhance antigen processing and presentation and also improve DC life span (34, 40), it may be useful to augment the protective effect of our DC-based vaccine against *C. gattii* infection.

Previous studies showed that T cells, particularly IFN-γ-producing T cells, were essential for protection against *C. neoformans* infection in mice (35, 36). IFN-γ production induced by *C. neoformans* infection enhanced the migration and killing capacity of

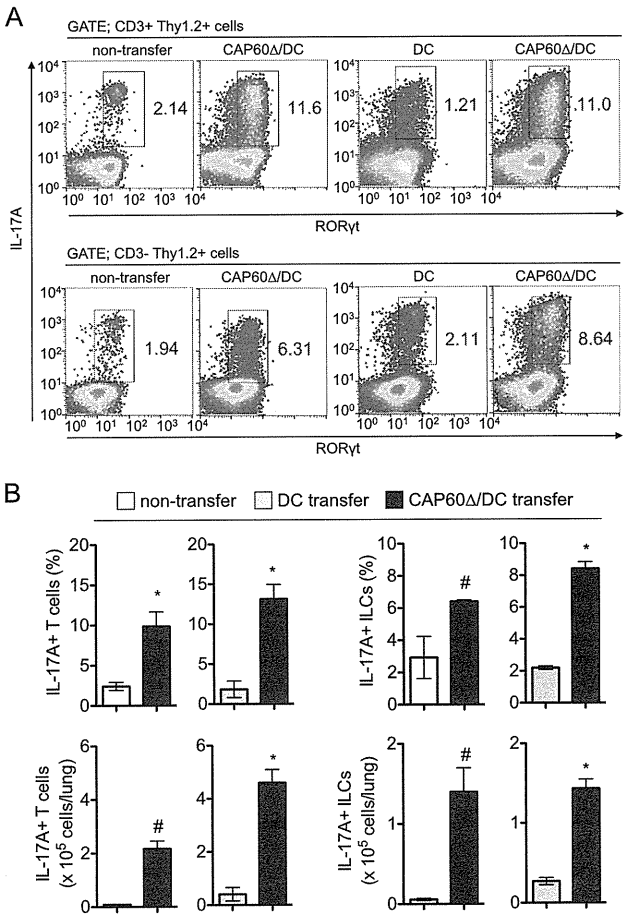


FIG 5 Transferring CAP60Δ/DCs induces IL-17A-producing cells in lungs. Lung leukocytes were obtained from three mice at 1 day after infection and were stimulated with PMA and ionomycin for 3 h. For flow cytometry analysis, gates were set for $CD3^+$ $Thy1.2^+$ cells or $CD3^-$ $Thy1.2^+$ cells. Representative flow cytometry profiles (A) and histograms for statistical analysis (B) from two independent experiments are shown. Results in histograms are means ± SDs. *, $P < 0.05$ versus control by unpaired *t* test; #, $P < 0.05$ versus control by unpaired *t* test with Welch's correction.

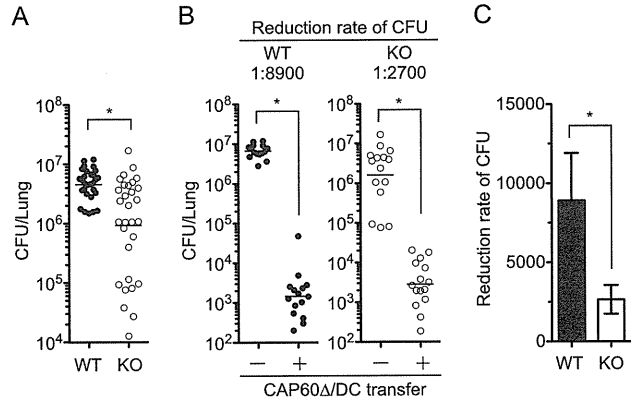


FIG 6 DC-based vaccine amelioration of the fungal burden is partially reduced in IFN-γ KO mice. (A) Fungal burdens in the lungs of C57BL/6J (WT) mice and IFN-γ KO mice were determined on days 9 to 14 postinfection. Data from six independent experiments were combined. (B and C) Vaccination and infection were performed as described in the legend to Fig. 2, and the fungal burden in lungs was determined on day 14 postinfection. Data from three independent experiments were combined. Vaccine effects between WT and KO mice were compared based on the reduced fungal burden rate (C). Panels A and B show dot plots with geometric means, and panel C shows means ± SEMs. *, $P < 0.05$ by Mann-Whitney U test.

macrophages (32, 41). Although transferring CAP60Δ/DCs strongly induced an IFN-γ response that was partially required for protection against *C. gattii*, this DC-based vaccine was still effective for inhibiting fungal growth in IFN-γ KO mice (Fig. 6). This suggested that both IFN-γ-dependent and IFN-γ-independent responses were involved in vaccine-induced protection against pulmonary infection with *C. gattii*.

The role of IL-17A in cryptococcosis is controversial. Several reports showed that IL-17A-producing CD4 T cells were increased in the lungs after pulmonary infection with *C. neoformans* (33, 42). Two reports indicated that IL-17A was dispensable for protection against pulmonary infection with *C. neoformans* (42, 43), while another report showed that IL-17A enhanced host defenses against pulmonary *C. neoformans* infection (33). It has also been shown that IL-17A was required for leukocyte accumulation, including numerous granulocytes, at the early phase of infection and for the development of MGCs that engulfed fungal cells at the late phase of *C. neoformans* infection. Thus, fungal clearance was impaired in IL-17A KO mice (33).

In our study, $IL\text{-}17A^+$ T cells and $IL\text{-}17A^+$ innate lymphoid cells (ILCs) increased in the lungs of immunized mice at day 1 postinfection (Fig. 5), and the fungal growth in mouse lungs was significantly suppressed at day 3 postinfection (Fig. 2). Additionally, the amount of IL-17A was also increased in the lungs of immunized mice at day 14 after infection (see Fig. S6 in the supplemental material). In agreement with previous findings that an IL-17A response induced neutrophil recruitment, the number of neutrophils increased in the lungs of immunized mice (see Fig. S5). Collectively, these results implied that IL-17A might contribute to vaccine-induced protection against pulmonary infection with highly virulent *C. gattii*. Further studies will be needed to determine the main factors of DC-based vaccine-induced immunity for protection against pulmonary infection with highly virulent *C. gattii*.

In summary, we demonstrated that transferring CAP60Δ/DCs strongly induced cytokine-producing CD4 T cells and MGCs that engulfed fungal cells and that this was associated with protection against pulmonary infection with highly virulent *C. gattii*. We propose that this DC-based vaccine is useful for (i) determining which antigens can induce cytokine-producing T cells and (ii) assessing those memory T cell responses that contribute to protection against highly virulent *C. gattii*. This may lead to the development of new means to control lethal *C. gattii* infections.

## ACKNOWLEDGMENTS

This work was supported by Health Science Research Grants for Research on Emerging and Re-emerging Infectious Diseases (H25-Shinkou-Shitei-001, H25-Shinkou-Shitei-002, H25-shinkou-Wakate-005, H25-Shinkou-Ippan-006, and H26-Shinkoujitsuyouka-Ippan-010) from the Ministry of Health, Labor and Welfare of Japan, by a grant from the Strategic Research Foundation Grant-aided Project for Private Schools at Heisei 23rd, KAKENHI (26860774), from the Ministry of Education, Culture, Sports, Science, and Technology of Japan, and by a grant from the Life Science Foundation of Japan.

## REFERENCES


1. Chen S, Sorrell T, Nimmo G, Speed B, Currie B, Ellis D, Marriott D, Pfeiffer T, Parr D, Byth K. 2000. Epidemiology and host- and variety-dependent characteristics of infection due to *Cryptococcus neoformans* in Australia and New Zealand. Australasian Cryptococcal Study Group. Clin Infect Dis **31**:499–508. http://dx.doi.org/10.1086/313992.
2. Galanis E, MacDougall L, Kidd S, Morshed M, British Columbia Cryptococcus gattii Working Group. 2010. Epidemiology of *Cryptococcus gattii*, British Columbia, Canada, 1999–2007. Emerging Infect Dis **16**:251–257. http://dx.doi.org/10.3201/eid1602.090900.
3. Smith RM, Mba-Jonas A, Tourdjman M, Schimek T, DeBess E, Marsden-Haug N, Harris JR. 2014. Treatment and outcomes among patients with *Cryptococcus gattii* infections in the United States Pacific Northwest. PLoS One **9**:e88875. http://dx.doi.org/10.1371/journal.pone.0088875.
4. BCCDC. 2011. Environmental pathogens, *Cryptococcus gattii*, p 112–113. British Columbia Annual Summary of Reportable Diseases 2011. BC Centre for Disease Control, Vancouver, BC, Canada. http://www.bccdc.ca/util/about/annreport/default.htm.
5. CDC. 2010. Emergence of *Cryptococcus gattii*, Pacific Northwest, 2004–2010. MMWR Morb Mortal Wkly Rep **59**:865–868.
6. Fraser JA, Giles SS, Wenink EC, Geunes-Boyer SG, Wright JR, Diezmann S, Allen A, Stajich JE, Dietrich FS, Perfect JR, Heitman J. 2005. Same-sex mating and the origin of the Vancouver Island *Cryptococcus gattii* outbreak. Nature **437**:1360–1364. http://dx.doi.org/10.1038/nature04220.
7. Ngamskulrungroj P, Chang Y, Sionov E, Kwon-Chung KJ. 2012. The primary target organ of *Cryptococcus gattii* is different from that of *Cryptococcus neoformans* in a murine model. mBio **3**(3):e00103-12. http://dx.doi.org/10.1128/mBio.00103-12.
8. Okubo Y, Wakayama M, Ohno H, Yamamoto S, Tochigi N, Tanabe K, Kaneko Y, Yamagoe S, Umeyama T, Shinozaki M, Nemoto T, Nakayama H, Sasai D, Ishiwatari T, Shimodaira K, Yamamoto Y, Kamei K, Miyazaki Y, Shibuya K. 2013. Histopathological study of murine pulmonary cryptococcosis induced by *Cryptococcus gattii* and *Cryptococcus neoformans*. Jpn J Infect Dis **66**:216–221. http://dx.doi.org/10.7883/yoken.66.216.
9. Cheng P-Y, Sham A, Kronstad JW. 2009. *Cryptococcus gattii* isolates from the British Columbia cryptococcosis outbreak induce less protective inflammation in a murine model of infection than *Cryptococcus neoformans*. Infect Immun **77**:4284–4294. http://dx.doi.org/10.1128/IAI.00628-09.
10. Einsiedel L, Gordon DL, Dyer JR. 2004. Paradoxical inflammatory reaction during treatment of *Cryptococcus neoformans var. gattii* meningitis in an HIV-seronegative woman. Clin Infect Dis **39**:e78–e82. http://dx.doi.org/10.1086/424746.
11. Brouwer AE, Siddiqui AA, Kester MI, Sigaloff KCE, Rajanuwong A, Wannapasni S, Chierakul W, Harrison TS. 2007. Immune dysfunction in HIV-seronegative, Cryptococcus *gattii* meningitis. J Infect **54**:e165–e168. http://dx.doi.org/10.1016/j.jinf.2006.10.002.
12. Springer DJ, Ren P, Raina R, Dong Y, Behr MJ, McEwen BF, Bowser SS, Samsonoff WA, Chaturvedi S, Chaturvedi V. 2010. Extracellular fibrils of pathogenic yeast *Cryptococcus gattii* are important for ecological niche, murine virulence and human neutrophil interactions. PLoS One **5**:e10978. http://dx.doi.org/10.1371/journal.pone.0010978.
13. Yauch LE, Lam JS, Levitz SM. 2006. Direct inhibition of T-cell responses by the *Cryptococcus* capsular polysaccharide glucuronoxylomannan. PLoS Pathog **2**:e120. http://dx.doi.org/10.1371/journal.ppat.0020120.
14. Steinman RM, Witmer MD. 1978. Lymphoid dendritic cells are potent stimulators of the primary mixed leukocyte reaction in mice. Proc Natl Acad Sci U S A **75**:5132–5136. http://dx.doi.org/10.1073/pnas.75.10.5132.
15. Palucka K, Banchereau J. 2013. Dendritic-cell-based therapeutic cancer vaccines. Immunity **39**:38–48. http://dx.doi.org/10.1016/j.immuni.2013.07.004.
16. García F, Climent N, Assoumou L, Gil C, González N, Alcamí J, León A, Romeu J, Dalmau J, Martínez-Picado J, Lifson J, Autran B, Costagliola D, Clotet B, Gatell JM, Plana M, Gallart T, DCV2/MANON07-AIDS Vaccine Research Objective Study Group. 2011. A therapeutic dendritic cell-based vaccine for HIV-1 infection. J Infect Dis **203**:473–478. http://dx.doi.org/10.1093/infdis/jiq077.
17. d'Ostiani CF, Del Sero G, Bacci A, Montagnoli C, Spreca A, Mencacci A, Ricciardi-Castagnoli P, Romani L. 2000. Dendritic cells discriminate between yeasts and hyphae of the fungus *Candida albicans*. Implications for initiation of T helper cell immunity *in vitro* and *in vivo*. J Exp Med **191**:1661–1674. http://dx.doi.org/10.1084/jem.191.10.1661.
18. Bozza S, Perruccio K, Montagnoli C, Gaziano R, Bellocchio S, Nkwanyuo G, Pitzurra L, Velardi A, Romani L. 2003. A dendritic cell vaccine against invasive aspergillosis in allogeneic hematopoietic transplantation. Blood **102**:3807–3814. http://dx.doi.org/10.1182/blood-2003-03-0748.
19. Roy RM, Klein BS. 2012. Dendritic cells in antifungal immunity and vaccine design. Cell Host Microbe **11**:436–446. http://dx.doi.org/10.1016/j.chom.2012.04.005.
20. Kidd SE, Hagen F, Tscharke RL, Huynh M, Bartlett KH, Fyfe M, Macdougall L, Boekhout T, Kwon-Chung KJ, Meyer W. 2004. A rare genotype of *Cryptococcus gattii* caused the cryptococcosis outbreak on Vancouver Island (British Columbia, Canada). Proc Natl Acad Sci U S A **101**:17258–17263. http://dx.doi.org/10.1073/pnas.0402981101.
21. Campbell LT, Currie BJ, Krockenberger M, Malik R, Meyer W, Heitman J, Carter D. 2005. Clonality and recombination in genetically differentiated subgroups of *Cryptococcus gattii*. Eukaryot Cell **4**:1403–1409. http://dx.doi.org/10.1128/EC.4.8.1403-1409.2005.
22. Fraser JA, Subaran RL, Nichols CB, Heitman J. 2003. Recapitulation of the sexual cycle of the primary fungal pathogen *Cryptococcus neoformans* var. *gattii*: implications for an outbreak on Vancouver Island, Canada. Eukaryot Cell **2**:1036–1045. http://dx.doi.org/10.1128/EC.2.5.1036-1045.2003.
23. Toffaletti DL, Rude TH, Johnston SA, Durack DT, Perfect JR. 1993. Gene transfer in *Cryptococcus neoformans* by use of biolistic delivery of DNA. J Bacteriol **175**:1405–1411.
24. Bahn Y-S, Hicks JK, Giles SS, Cox GM, Heitman J. 2004. Adenylyl cyclase-associated protein AcaI regulates virulence and differentiation of *Cryptococcus neoformans* via the cyclic AMP-protein kinase A cascade. Eukaryot Cell **3**:1476–1491. http://dx.doi.org/10.1128/EC.3.6.1476-1491.2004.
25. Simon DM, Tsai LW, Ingenito EP, Starcher BC, Mariani TJ. 2010. PPARgamma deficiency results in reduced lung elastic recoil and abnormalities in airspace distribution. Respir Res **11**:69. http://dx.doi.org/10.1186/1465-9921-11-69.
26. Carvalho NB, Oliveira FS, Durães FV, de Almeida LA, Flórido M, Prata LO, Caliari MV, Appelberg R, Oliveira SC. 2011. Toll-like receptor 9 is required for full host resistance to *Mycobacterium avium* infection but plays no role in induction of Th1 responses. Infect Immun **79**:1638–1646. http://dx.doi.org/10.1128/IAI.01030-10.
27. Siegemund S, Alber G. 2008. *Cryptococcus neoformans* activates bone marrow-derived conventional dendritic cells rather than plasmacytoid dendritic cells and down-regulates macrophages. FEMS Immunol Med Microbiol **52**:417–427. http://dx.doi.org/10.1111/j.1574-695X.2008.00391.x.
28. Vecchiarelli A, Pietrella D, Lupo P, Bistoni F, McFadden DC, Casadevall A. 2003. The polysaccharide capsule of *Cryptococcus neoformans* interferes with human dendritic cell maturation and activation. J Leukoc Biol **74**:370–378. http://dx.doi.org/10.1189/jlb.1002476.
29. Fromtling RA, Kaplan AM, Shadomy HJ. 1983. Immunization of mice with stable, acapsular, yeast-like mutants of *Cryptococcus neoformans*. Sabouraudia **21**:113–119. http://dx.doi.org/10.1080/00362178385380181.
30. Hill JO. 1992. CD4+ T cells cause multinucleated giant cells to form around *Cryptococcus neoformans* and confine the yeast within the primary site of infection in the respiratory tract. J Exp Med **175**:1685–1695. http://dx.doi.org/10.1084/jem.175.6.1685.
31. Wozniak KL, Ravi S, Macias S, Young ML, Olszewski MA, Steele C, Wormley FL. 2009. Insights into the mechanisms of protective immunity against *Cryptococcus neoformans* infection using a mouse model of pulmonary cryptococcosis. PLoS One **4**:e6854. http://dx.doi.org/10.1371/journal.pone.0006854.
32. Kawakami K, Qureshi MH, Zhang T, Koguchi Y, Shibuya K, Naoe S, Saito A. 1999. Interferon-gamma (IFN-gamma)-dependent protection and synthesis of chemoattractants for mononuclear leucocytes caused by IL-12 in the lungs of mice infected with *Cryptococcus neoformans*. Clin Exp Immunol **117**:113–122. http://dx.doi.org/10.1046/j.1365-2249.1999.00955.x.
33. Murdock BJ, Huffnagle GB, Olszewski MA, Osterholzer JJ. 2014. Interleukin-17A enhances host defense against cryptococcal lung infection through effects mediated by leukocyte recruitment, activation, and gamma interferon production. Infect Immun **82**:937–948. http://dx.doi.org/10.1128/IAI.01477-13.
34. Jagannath C, Lindsey DR, Dhandayuthapani S, Xu Y, Hunter RL, Eissa

NT. 2009. Autophagy enhances the efficacy of BCG vaccine by increasing peptide presentation in mouse dendritic cells. Nat Med 15:267–276. http://dx.doi.org/10.1038/nm.1928.
35. **Huffnagle GB, Lipscomb MF, Lovchik JA, Hoag KA, Street NE.** 1994. The role of CD4+ and CD8+ T cells in the protective inflammatory response to a pulmonary cryptococcal infection. J Leukoc Biol 55:35–42.
36. **Kawakami K.** 2004. Regulation by innate immune T lymphocytes in the host defense against pulmonary infection with *Cryptococcus neoformans*. Jpn J Infect Dis 57:137–145.
37. **Chaturvedi AK, Hameed RS, Wozniak KL, Hole CR, Leopold Wager CM, Weintraub ST, Lopez-Ribot JL, Wormley FL.** 2014 Vaccine-mediated immune responses to experimental pulmonary *Cryptococcus gattii* infection in mice. PLoS One 9:e104316. http://dx.doi.org/10.1371/journal.pone.0104316.
38. **Huston SM, Li SS, Stack D, Timm-McCann M, Jones GJ, Islam A, Berenger BM, Xiang RF, Colarusso P, Mody CH.** 2013. *Cryptococcus gattii* is killed by dendritic cells, but evades adaptive immunity by failing to induce dendritic cell maturation. J Immunol 191:249–261. http://dx.doi.org/10.4049/jimmunol.1202707.
39. **Goldman DL, Lee SC, Mednick AJ, Montella L, Casadevall A.** 2000. Persistent *Cryptococcus neoformans* pulmonary infection in the rat is associated with intracellular parasitism, decreased inducible nitric oxide synthase expression, and altered antibody responsiveness to cryptococcal polysaccharide. Infect Immun 68:832–838. http://dx.doi.org/10.1128/IAI.68.2.832-838.2000.
40. **Amiel E, Everts B, Freitas TC, King IL, Curtis JD, Pearce EL, Pearce EJ.** 2012. Inhibition of mechanistic target of rapamycin promotes dendritic cell activation and enhances therapeutic autologous vaccination in mice. J Immunol 189:2151–2158. http://dx.doi.org/10.4049/jimmunol.1103741.
41. **Flesch IE, Schwamberger G, Kaufmann SH.** 1989. Fungicidal activity of IFN-gamma-activated macrophages. Extracellular killing of *Cryptococcus neoformans*. J Immunol 142:3219–3224.
42. **Yamamoto H, Nakamura Y, Sato K, Takahashi Y, Nomura T, Miyasaka T, Ishii K, Hara H, Yamamoto N, Kanno E, Iwakura Y, Kawakami K.** 2014. Defect of CARD9 leads to impaired accumulation of gamma interferon-producing memory phenotype T cells in lungs and increased susceptibility to pulmonary infection with *Cryptococcus neoformans*. Infect Immun 82:1606–1615. http://dx.doi.org/10.1128/IAI.01089-13.
43. **Hardison SE, Wozniak KL, Kolls JK, Wormley FL.** 2010. Interleukin-17 is not required for classical macrophage activation in a pulmonary mouse model of *Cryptococcus neoformans* infection. Infect Immun 78:5341–5351. http://dx.doi.org/10.1128/IAI.00845-10.

J Infect Chemother 21 (2015) 837–841

Contents lists available at ScienceDirect

Journal of Infection and Chemotherapy

journal homepage: http://www.elsevier.com/locate/jic

Original article

# Risk factors for and circumstances of needlestick and sharps injuries of doctors in operating rooms: A study focusing on surgeries using general anesthesia at Kurume University Hospital, Japan

Yuko Yonezawa [a, 1], Koji Yahara [b, *, 1], Miho Miura [c], Fumiyo Hieda [c], Ryoji Yamakawa [d, e], Kenji Masunaga [c, f], Yasunori Mishima [d, g], Hiroshi Watanabe [c, f]

[a] Division of Biostatistics, Kurume University School of Medicine, Kurume, Fukuoka 830-0011, Japan
[b] Biostatistics Center, Kurume University School of Medicine, Kurume, Fukuoka 830-0011, Japan
[c] Division of Infection Control and Prevention, Kurume University Hospital, Kurume, Fukuoka 830-0011, Japan
[d] Central Division of Surgeries, Kurume University Hospital, Kurume, Fukuoka 830-0011, Japan
[e] Department of Ophthalmology, Kurume University School of Medicine, Kurume, Fukuoka 830-0011, Japan
[f] Department of Infection Control and Prevention, Kurume University School of Medicine, Kurume, Fukuoka 830-0011, Japan
[g] Department of Anesthesiology, Kurume University, Kurume, Fukuoka 830-0011, Japan

ARTICLE INFO

*Article history:*
Received 6 April 2015
Received in revised form
13 August 2015
Accepted 19 August 2015
Available online 14 October 2015

*Keywords:*
Needlestick and sharps injury
Operating rooms
Surgery
Infection control
Epidemiology
General anesthesia

ABSTRACT

Healthcare workers are exposed to serious infectious diseases via needlestick and sharps injuries. The operating room is a particularly important environment in which the risk for needlestick injuries is increased for surgical doctors. According to national surveillance studies, the proportion of needlestick and sharps injuries in operating rooms has been increasing for unknown reasons. In this study, we examined risk factors for and circumstances of injuries in operating rooms by combining and analyzing incidence reports and electronic records of every surgery in Kurume University Hospital (Kurume, Japan). The annual injury rate (reflecting the reporting rate) rose continuously from fiscal years 2007–2012. We conducted analyses focusing on surgeries that used general anesthesia, which accounted for 88.1% of the injuries. An analysis of the time of injury found that the number of injuries increased toward the end of the surgical procedure. A comparative analysis of surgeries by doctors who had experienced injury revealed risk for the injury increased when a procedure ended after 20:00. In addition, a comparative analysis of doctors with and without injury experience who had similar level of operating time per year revealed that the number of working years was not lower in the injured doctors. Although the data analyzed in this study were confined to one university hospital, our approach and these results will form a basis on which to consider more effective measures to prevent injury in operating rooms.



## 1. Introduction

Needlestick and sharps injuries pose serious risk for occupational transmission of bloodborne viruses to healthcare workers. The injury can cause transmission of at least 20 different pathogens, including hepatitis B and C viruses and human immunodeficiency virus [1]. Every year, these types of injuries expose hundreds of thousands of healthcare workers to deadly viruses [2]. They also cause anxiety and depression [3] or mental illness with a severity similar to other psychiatric traumas [4]. Costs of post-exposure treatment of injured workers (e.g., laboratory tests, medications, counseling, and medical services) have become an economic burden in many countries, and the importance of more aggressive and comprehensive preventive measures has been noted [5].

The operating room is a particularly important environment in which the risk for injury to surgical doctors is increased [6]. The environment is "blood-intensive, requires extensive manipulation of sharp instruments, often with compromised visual cues, and involves highly orchestrated interactions among members of the surgical team" [6]. The frequency of reported injuries occurring in the operating room is second only to those occurring in patients'

* Corresponding author. Tel.: +81 942 31 7835; fax: +81 942 31 7865.
*E-mail address:* koji_yahara@med.kurume-u.ac.jp (K. Yahara).
[1] Contributed equally to this article.

http://dx.doi.org/10.1016/j.jiac.2015.08.012
1341-321X/

rooms [2,7,8]. An analysis of injury surveillance data from 87 hospitals in the United States from 1993 through 2006 revealed that injury rates in the operating room actually increased after legislation of the Needlestick Safety and Prevention Act in 2000 [6]. The authors discussed the possibility that the surgical setting has been more unresponsive to the law than other locations within the hospital. Similarly, national surveillance studies in Japan revealed an increase in the proportion of needlestick and sharps injuries in operating rooms from 1996 to 2012, but the reasons for the increase were unknown [9].

An observational study of surgeries performed during a 2-month period in operating rooms in San Francisco General Hospital recorded descriptions of exposures to blood or another body fluids (including via needlestick injury) and found that surgeries lasting >3 h, blood loss >300 mL, and major vascular and intra-abdominal gynecologic surgeries were main risk factors for the exposures [10]. A study that explored risk factors for sharps-related blood and body fluid exposure in operating rooms at Duke University Medical Center reported an increase in the number of personnel working in the surgical field as a new risk factor, in addition to the increase in blood loss and operating time [11].

These related studies, however, did not specifically focus on the needlestick and sharps injuries in operating rooms. Thus, it remains unknown whether the risk factors for blood and body fluid exposures have significant effect if the focus is specifically on exposures caused by needlestick and sharps injuries. More direct, unanswered questions include the following: During surgical procedures, is there a time period in which there is an increased risk for these types of injuries? Is the risk for injury increased in a surgery ending at night? Is the risk related to the work environment or condition of the healthcare workers (e.g., workloads before a surgery, number of working years, or total time of surgeries per person per year)?

To answer these questions, we explored risk factors for and circumstances of needlestick and sharps injuries in operating rooms. We combined and analyzed incidence reports and electronic records of every surgery performed in Kurume University Hospital (Kurume, Japan).

## 2. Materials and methods

### 2.1. Data

We obtained electronic records of every surgery conducted from January 1, 2006, to March 31, 2013, in Kurume University Hospital with 25 diagnosis and treatment departments and 24 wards with 1025 beds. We also obtained injury report data during the same period (it is a rule in the hospital that an injured medical worker must send a report to the Division of Infection Control and Prevention). Most of the injuries (57.1%) occurred in doctors, followed by nurses (39.3%) and other medical workers (3.6%). In this study, we focus on injures of doctors that account for the majority. The "doctor" here refers to a surgeon or physician working in the operating room at the time of a surgical procedure (except for students and residents). The total number of reported injuries was 63, from which we calculated an annual injury rate, as discussed in Section 2.2.

We were able to find a corresponding electronic record of a surgery for 42 of the 63 injuries, and these revealed that most (37 of 42; 88.1%) were surgeries that used general anesthesia and took a mean of 5.3 h to perform. The time required for surgical procedures not involving general anesthesia was much shorter (mean, 1.4 h). Because risk factors for and circumstances of the needlestick and sharps injuries are expected to be quite different between surgeries with and without general anesthesia, we focused on the former, except for the calculation of annual injury rate.

To measure years of experience for every doctor, we obtained from the division of personnel at Kurume University data on the number of working years of the doctors involved in the surgeries during the study period. The data indicate the number of years each doctor has worked since start of their post at Kurume University until April 2014.

### 2.2. Annual injury rate

We calculated the annual injury rate as the number of doctors injured divided by the total number of doctors involved in all operations (with or without general anesthesia) during each fiscal year of the study period. No doctor experienced the injury twice or more in a single fiscal year.

### 2.3. Relationship between injury occurrence and time

We first classified the injuries by time of injury occurrence during a surgery (time zone): time zone I: after entering an operating room and before start of a surgical procedure; time zone II: after the start of a surgery and before one-third of the total time had passed; time zone III: after one-third of the procedure time had passed and before two-thirds had passed; time zone IV: after two-thirds of the time had passed and before the end of a surgery; and time zone V: after the end of a surgery and before exit from an operating room. We then subclassified the injuries that happened in time zones II–IV (i.e., from the start to the end of a surgery) in terms of operating time. We used four time categories of 200 min each: 0–199 min, 200–399 min, 400–599 min, and $\geq$600 min.

### 2.4. Comparative analysis of surgeries by doctors with injury experience

We considered potential risk factors for the needlestick and sharps injuries as follows: total operating time during 1 week before the surgery or of up to the 7 latest surgeries within the past 6 months (as a factor of a doctor's workload), operating time of the surgery, and surgeries ending after 20:00. To evaluate these factors, it was necessary to account for individual differences among the doctors (e.g., in terms of experience, specialty, and frequency of surgeries). For that purpose, we took a 1:3 matching approach in which for each "case" surgery causing the injury, we randomly selected three "control" surgeries performed by the same doctor before the case surgery. To make the background of the case and control surgery data as similar as possible, we selected 3 from the 10 latest surgeries in which the role of the doctor (operator, assistant, anesthesiologist, or doctor in charge) and sex of patients were the same as those of the case surgery. We were able to use the surgery data of 24 injured doctors that satisfied the matching criteria.

We evaluated the potential risk factors by applying conditional logistic regression to the 1:3 matched data. We used the R statistical software version 3.1.2 and the survival package [12]. We used a less stringent significance level (10%) because the sample size was small and we wanted to prioritize reduction of false-negative results when we evaluated risk factors for detrimental events such as the needlestick and sharps injuries.

### 2.5. Comparative analysis of doctors with and without injury experience

We conducted a comparative analysis of doctors with and without injury experience. We focused on doctors who used general anesthesia in >50% of surgeries they performed. For every

doctor with injury experience, we selected one doctor without it as a control who had similar level of operating time per year. This is because it is expected that the longer the operating time per year, the higher the risk of the injury, which should be adjusted in advance to compare the doctors. We used box plots and the Wilcoxon rank-sum test to compare among them the number of working years.

### 2.6. Ethics

The study was approved by the ethics committee of Kurume University (approval number 14070).

## 3. Results

Calculation of the annual injury rate revealed a continuous increase in the rate from fiscal year 2007–2012 (Fig. 1). The raw number of incidence reports or injured doctors in each fiscal year is shown in Fig. S1. During the study period, there was no substantial increase or decrease in the total number of surgeries and doctors involved in the surgeries in each fiscal year (Figs. S2 and S3). During that period, there were two hospital departments that had more than 4 incidence reports: department of surgery (42.9%) and that of urology (16.7%), the proportion of which was significantly higher than that among all surgeries (19.1% and 6.4%, $p = 0.03$ and $p = 0.02$ by Chi-square test, respectively).

The analysis of timing of the injury in the surgeries revealed that the number of injuries increased when the surgeries approached their end (Fig. 2a): 7 injuries occurred after the start of a surgery and before one-third of the procedure time had passed; 9 injuries occurred after one-third of the time had passed and before two-thirds of the time had passed; and 14 injuries occurred after two-thirds of the procedure time had passed and before the end of the surgery. The numbers of injuries before the start and after the end of a surgery in the operation room were 3 and 4, respectively, which were less than that during the surgery. The subclassification of the injuries that occurred during a surgery in terms of actual operating time did not show any notable trend (Fig. 2b).

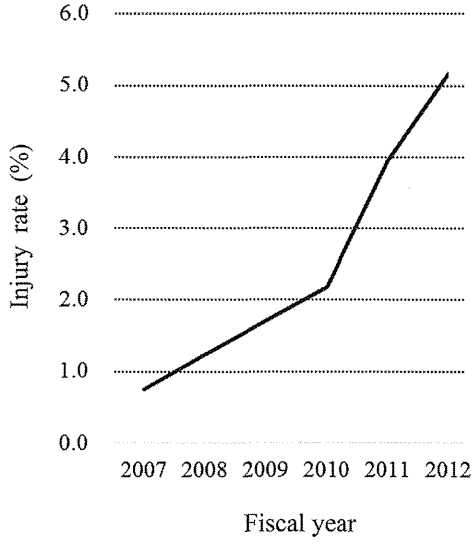


**Fig. 1.** Annual rate of needlestick and sharps injuries. The injury rate (y axis) was determined using the following equation: (the number of injured doctors)/(total number of doctors involved in operations in the fiscal year) × 100.

The comparative analysis of surgeries by doctors with injury experience revealed that risk for the injury increased when a surgery ended after 20:00 ($p = 0.099$) (Table 1). The other potential risk factors (operating time of a surgery and total operating time during 1 week before the surgery or of up to the 7 latest surgeries within past 6 months) were not statistically significant ($p > 0.1$).

The personnel records of doctors' tenure at the hospital correlated well with the years of experience given in the injury reports (Pearson correlation coefficient, 0.76). We compared the number of working years between doctors with and without injury experience by using a matched dataset in which operating time per year is controlled to be equal (228 h on average) in both of the groups. The number of working years had almost no correlation with the operating time per year (Pearson correlation coefficient, 0.03). The analysis showed that average and median of the working years were slightly higher in the former (13.5 vs 10.3 and 13 vs 11, respectively) (Fig. 3), although the difference was not statistically significant ($p = 0.18$, Wilcoxon rank-sum test).

## 4. Discussion

In this study, we showed a continuous increase in the annual rate of needlestick and sharps injuries in our hospital's operating rooms from fiscal year 2007–2012. During that period, in April 2010, the hospital introduced a new instruction manual and an inspection kit for injury. It also initiated preventive measures (e.g., introduction of a safety zone in an operating room) directed by a working group, in May 2012. It is expected that these measures caused change in practice and awareness among surgical doctors and an increase in reporting rates, which has been estimated to be quite low (e.g., 2.26%, according to a study at a district general hospital in the United Kingdom [13]).

The increase in the number of injuries when the surgeries approached their end (in the time zone III and IV) is the first such finding reported in studies of needlestick and sharps injuries in the operating room. We made the finding possible by combining the data of incidence reports and electronic records of every surgery in the hospital.

Our finding that risk for injury increased when a surgery ended after 20:00 is also the first such finding reported in a study of injuries occurring in the operating room. In Kurume University Hospital during the study period, the number of nurses (indirect assistants) was reduced in surgeries ending later at night, and this may be related to the increased risk for the injury.

Meanwhile, proportion of injuries in the time zone IV (or III and IV) compared to other injuries did not show significant increase from fiscal year 2007–2012 ($p = 0.63$ (or 0.59), by Fisher's exact test). Proportion of surgeries ending after 20:00 compared to other surgeries also did not show significant increase during that period ($p = 0.25$, by Chi-square test). Therefore, these are not factors of the apparent continuous increase in the annual rate of needlestick and sharps injuries in our hospital, which is rather explained by the increase in reporting rates.

The mean number of working years was slightly higher in the injured doctors than in the other doctors (Fig. 3), although the difference was not significant. This may be counterintuitive because one might think doctors with less experience would be subject to more injuries. A possible explanation is that doctors with more experience are assigned to more surgeries than other doctors, which would increase their opportunities for injury in the operation room. Another study in another hospital is required to investigate whether this is a general phenomenon.

Among the limitations of the present study is that, due to absence of data, we did not examine the effect of the number of needles used in a surgery, or of a specific type of surgery or needle.

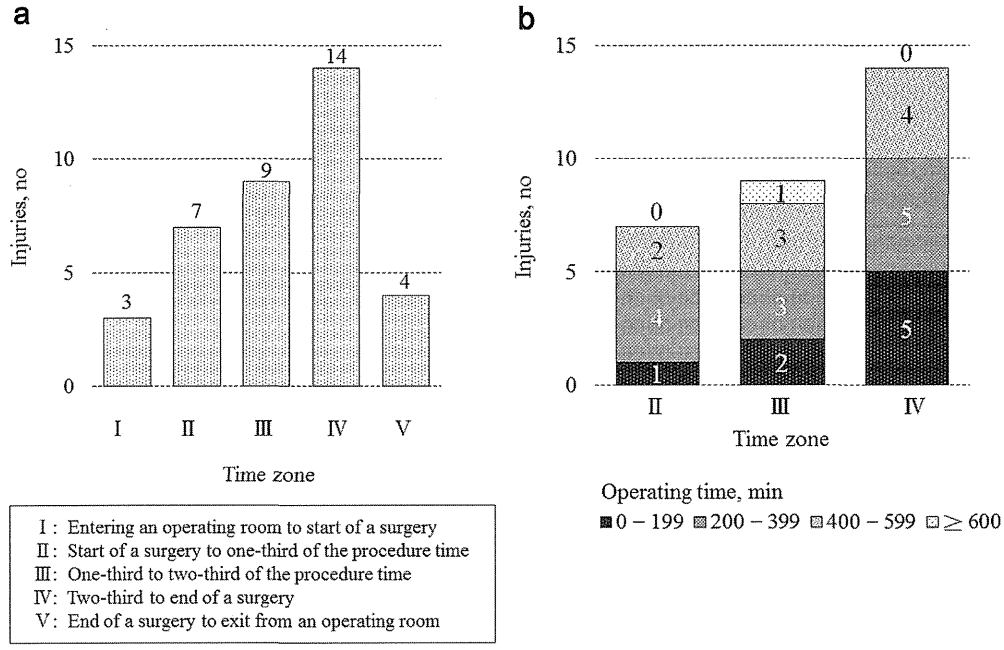


**Fig. 2.** (a) Classification of the injuries according to timing in a surgery (time zone). (b) Subclassification according to operating time of a surgery. The injuries that occurred during the time from the start to the end of a surgery (time zones II–IV) were subclassified into four categories of operating time of a surgery.

**Table 1**
Examination of risk factors by univariate conditional logistic regression.

| Risk factor | OR | 90% CI | *p* value | Injured: others[a] |
|---|---|---|---|---|
| Total operating time during 1 week before the surgery | 1.00 | 0.89–1.13 | 0.97 | 2.9 (3.8): 2.9 (3.9)[b] |
| Total operating time of up to the 7 latest surgeries within past 6 months | 1.05 | 0.98–1.12 | 0.20 | 28.1 (13.9): 26.1 (13.7)[b] |
| Operating time of surgical procedure | 1.07 | 0.94–1.23 | 0.37 | 5.0 (3.1): 4.4 (3.0)[b] |
| Surgeries ending after 20:00 | 4.50 | 1.01–20.11 | 0.099 | 12.5%: 2.8% |

The unit of time is hour; CI = confidence interval; OR = odds ratio.
[a] The number of operations with and without injuries is 24: 72.
[b] Mean (SD).

Similarly, we did not have direct data on doctors' workloads, such as off-the-clock work or work on the day after a night on duty. It is desirable to collect and analyze these data to deepen our understanding of risk factors for these types of injuries.

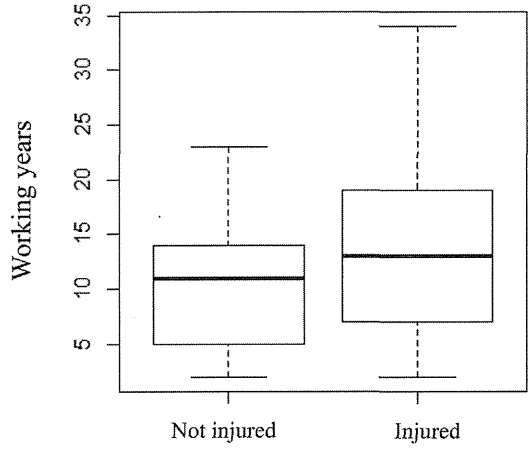


**Fig. 3.** Comparison of doctors with and without injury experience who had similar level of operating time per year in term of working years. The line in each box indicates the median, and the bottom and top of the box indicate the 25th and 75th percentiles.

A fundamental limitation of the present study is that the analyzed data were confined to one university hospital, which is expected to be biased. It is thus not possible to generalize and relate the results of the present study to those of the national surveillance studies that cover various hospitals across Japan. We hope that the present study will be a basis of future studies of various hospitals in Japan, which will altogether lead to elucidation of factors of the increase in the proportion of needlestick and sharps injuries in operating rooms reported in the national surveillance studies.

In April 2014, the working group in Kurume University Hospital started to show a DVD to surgical doctors about the risk for needlestick and sharps injuries in the operating room. Preliminary data show the number of injuries decreased after these viewings. Whether the measure was significantly effective will be examined after several years of surveillance.

To our knowledge, this is the first study to examine risk factors for and circumstances of needlestick and sharps injuries in surgeries using general anesthesia. In order to reduce the injuries, at least in Kurume University hospital, it will be effective to call surgical doctors' attention to the higher risk of injuries when the surgeries approach their end irrespective of their working years. The results are a basis on which to consider more effective preventive measures that should be carried out by all surgical doctors, including those with high levels of experience.

## Conflict of interest

None.

## Acknowledgments

The authors acknowledge the staff of the Division of Infection Control and Prevention and the Central Division of Surgeries, Kurume University Hospital.

## Appendix A. Supplementary data

Supplementary data related to this article can be found at http://dx.doi.org/10.1016/j.jiac.2015.08.012.

## References

[1] Beltrami EM, Williams IT, Shapiro CN, Chamberland ME. Risk and management of blood-borne infections in health care workers. Clin Microbiol Rev 2000;13:385–407.
[2] Nagao Y, Baba H, Torii K, Nagao M, Hatakeyama K, Iinuma Y, et al. A long-term study of sharps injuries among health care workers in Japan. Am J Infect Control 2007;35:407–11.
[3] Sohn JW, Kim BG, Kim SH, Han C. Mental health of healthcare workers who experience needlestick and sharps injuries. J Occup Health 2006;48:474–9.
[4] Green B, Griffiths EC. Psychiatric consequences of needlestick injury. Occup Med (Lond) 2013;63:183–8.
[5] Oh HS, Yoon Chang SW, Choi JS, Park ES, Jin HY. Costs of postexposure management of occupational sharps injuries in health care workers in the Republic of Korea. Am J Infect Control 2013;41:61–5.
[6] Jagger J, Berguer R, Phillips EK, Parker G, Gomaa AE. Increase in sharps injuries in surgical settings versus nonsurgical settings after passage of national needlestick legislation. J Am Coll Surg 2010;210:496–502.
[7] Jagger J, Perry J, Puro V, Ippolito G. Occupational exposure to bloodborne pathogens: epidemiology and prevention. In: Wenzel R, editor. Prevention and control of nosocomial infections. Philadelphia, PA: Lippincott Williams & Wilkins; 2003.
[8] Yoshikawa T, Wada K, Lee JJ, Mitsuda T, Kidouchi K, Kurosu H, et al. Incidence rate of needlestick and sharps injuries in 67 Japanese hospitals: a national surveillance study. PLoS One 2013;8:e77524.
[9] The Research Group of Occupational Infection Control and Prevention in Japan. Summary of the 2013 survey conducted by the Japan-EPINet Survey Working Group (JESWG2013). 2013.
[10] Gerberding JL, Littell C, Tarkington A, Brown A, Schecter WP. Risk of exposure of surgical personnel to patients' blood during surgery at San Francisco General Hospital. N Engl J Med 1990;322:1788–93.
[11] Myers DJ, Epling C, Dement J, Hunt D. Risk of sharp device-related blood and body fluid exposure in operating rooms. Infect Control Hosp Epidemiol 2008;29:1139–48.
[12] Therneau T. A package for survival analysis in S. 1999.
[13] Au E, Gossage JA, Bailey SR. The reporting of needlestick injuries sustained in theatre by surgeons: are we under-reporting? J Hosp Infect 2008;70:66–70.

INTERNAL MEDICINE

□ ORIGINAL ARTICLE □

# Potential Drug Interaction between Warfarin and Linezolid

Yoshiro Sakai[1,2], Tetsuya Naito[1], Chiyoko Arima[1], Miho Miura[3], Liang Qin[2], Hidenobu Hidaka[2,3], Kenji Masunaga[2,3], Tatsuyuki Kakuma[4] and Hiroshi Watanabe[2,3]

## Abstract

**Objective** Warfarin is known to interact with many drugs; however, there are currently no descriptions of an interaction with linezolid in the literature. It was recently brought to our attention, however, that several warfarin-medicated patients have experienced an increase in the prothrombin time international normalized ratio (PT-INR) following the administration of linezolid. We therefore performed a retrospective survey in order to investigate the possibility of an interaction between warfarin and linezolid.

**Methods** The survey items included age, gender, underlying disease, type of surgery, type of infectious disease, duration of linezolid administration, laboratory values and the dose of warfarin. The PT-INR was observed over time before treatment and at days 4 or 5 and 10, completion and one week after the end of concomitant therapy.

**Patients** The subjects included six patients who were recovering from recent heart-related surgery.

**Results** The PT-INR increased from 1.62±0.32 before concomitant linezolid administration to 3.00±0.83 at day 4 or 5 after concomitant administration ($p<0.01$) and significantly decreased from 1.65±0.45 at the completion of the regimen to 1.26±0.1 one week later ($p<0.05$). With respect to the relationship between the dose of warfarin and the PT-INR in five cases, the PT-INR increased following concomitant linezolid treatment in all cases.

**Conclusion** Although it has been reported that linezolid does not influence the metabolism or protein binding of warfarin, our data showed potential drug interactions between warfarin and linezolid. Our data suggest that PT-INR monitoring after the completion of concomitant warfarin and linezolid therapy is important.

**Key words:** warfarin, linezolid, drug interaction, PT-INR

**(Intern Med 54: 459-464, 2015)**
**(DOI: 10.2169/internalmedicine.54.3146)**

## Introduction

Warfarin does not directly act on coagulation factors present in the circulation, but rather exerts anticoagulant and thrombus formation-preventing effects by inhibiting the protein synthesis of vitamin K-dependent coagulation factor in the liver, and is used to treat and prevent both myocardial infarction and pulmonary embolism (1). However, warfarin is known to interact with various drugs, although the mechanism of interaction remains unclear in many cases, and not all drug combinations have been investigated. Therefore, it is necessary to pay close attention to changes in the patient's coagulative ability when concomitantly adding or withdrawing other drugs during anticoagulant therapy (2).

Linezolid is an oxazolidinone antibiotic that displays an antimicrobial activity against Gram-positive cocci, including resistant bacteria, such as methicillin-resistant *Staphylococcus aureus* (MRSA) (3). Linezolid exhibits a superior capacity for tissue transfer (4) and is expected to be efficacious in cases of infections that were previously difficult to treat due to problems in drug transfer. Linezolid is afforded an important status in the treatment guidelines for MRSA infection established by the Infectious Diseases Society of America (IDSA) in February 2011 (5).

Warfarin reportedly interacts with many antibiotics, as de-

[1]Department of Pharmacy, Kurume University Hospital, Japan, [2]Department of Infection Control and Prevention, Kurume University School of Medicine, Japan, [3]Division of Infection Control and Prevention, Kurume University Hospital, Japan and [4]Biostatistics Center, Kurume University School of Medicine, Japan

Received for publication April 22, 2014; Accepted for publication July 13, 2014

Correspondence to Dr. Yoshiro Sakai, sakai_yoshirou@kurume-u.ac.jp

**Table 1. Patient Background**

| Case number | Age | Gender | Underlying disease | Body weight (kg) | Surgery | Infectious disease | Causative organism | Linezolid starting day | Duration of linezolid administration (day) |
|---|---|---|---|---|---|---|---|---|---|
| Case 1 | 63 | Male | Mitral insufficiency | 64.2 | Valvoplasty | Infectious endocarditis | MRSA | 13 days postoperation | 50 |
| Case 2 | 40 | Male | Mitral insufficiency | 67.7 | Valve replacement (artificial valve) | Graft infection | Unclear | about 10 years after the surgery | 19 |
| Case 3 | 78 | Male | Mitral insufficiency | 52.7 | Valve replacement (biological valve) | Infectious endocarditis | Streptococcus constellatus | 8 days postoperation | 9 |
| Case 4 | 62 | Female | Mitral insufficiency | 46.1 | Valvoplasty | Infectious endocarditis | MRSE | 21 days postoperation | 33 |
| Case 5 | 69 | Male | Acute aortic dissection | 77.6 | Root replacement | Mediastinitis | MRSE | 14 days postoperation | 25 |
| Case 6 | 59 | Female | Mitral insufficiency | 59.3 | Valve replacement (artificial valve) | Infectious endocarditis | α-Streptococcus | 3 days preoperation | 28 |

scribed above, and attention must be paid to the potential for hemorrhagic complications (6). However, there are currently no descriptions of an interaction between warfarin and linezolid on the interview forms for either drug (2, 3). We encountered several patients who experienced an increase in the prothrombin time international normalized ratio (PT-INR) while receiving simultaneous treatment with warfarin and linezolid after cardiovascular surgery. We thus retrospectively surveyed patients who had simultaneously been treated with warfarin and linezolid and investigated the possibility of drug interactions based on changes in the PT-INR values, concomitantly administered drugs and/or the dose of warfarin in order to clarify possible interactions between these two drugs.

## Materials and Methods

### *Ethical approval*

All studies described herein were approved by the Human Ethics Review Board of Kurume University (13094).

### *Survey period and subjects*

The subjects included patients who has simultaneously been treated with warfarin and linezolid between January and December, 2011 at Kurume University Hospital. Patients already being treated with drugs known to influence the PT-INR when concomitantly administered with warfarin were excluded from the study.

### *Survey items and methods*

In order to investigate the occurrence of drug interactions in patients simultaneously treated with warfarin and linezolid, the subjects' electronic medical records were retrospectively surveyed. The survey items included age, gender, body weight, underlying disease, type of surgery, type of infectious disease, duration of linezolid administration, laboratory values [aspartate aminotransferase (AST), alanine aminotransferase (ALT), blood urea nitrogen (BUN), serum creatinine (Scr), serum albumin (Alb) and PT-INR], the dose of warfarin and concomitantly administered drugs. The laboratory values, excluding the PT-INR, were compared with respect to the following four time points of concomitant administration: before treatment, during treatment (at the time of the highest PT-INR), at the completion of treatment and one week after the completion of treatment. The PT-INR was observed over time before therapy and at days 4 or 5 and 10, completion and one week after the completion of concomitant therapy. There was a change in the measurement protocol for determining the PT-INR after a few years. Therefore, a post-surgery group that did not receive concomitant treatment with linezolid for mitral insufficiency was investigated for comparison purposes.

We defined the start date of linezolid therapy as day 0 and investigated changes in the dose of warfarin and the PT-INR from before treatment to five days after treatment.

### *Statistical analysis*

The laboratory data are presented as the mean ± standard deviation, and were compared using a paired t-test, with the significance level set at less than 5%.

The JMP10 software program (SAS Institute, Inc., Cary, USA) was used for the statistical analysis.

## Results

Six of the seven patients who had been simultaneously treated with warfarin and linezolid during the survey period were investigated in detail. One patient was excluded due to being previously treated with rifampicin, which reduces the effect of warfarin. That patient's background characteristics are shown in Table 1. The mean age of the six patients was 61.8±12.6 years. There were four men and two women, with a body weight of 61.3±11.2 kg, all of whom had undergone heart-related surgery. Linezolid was indicated for heart-related infection, and resistant bacteria were detected as the etiologic microorganism in half of these cases, with the most infectious form, endocarditis, being detected in four cases. The administration of anticoagulant therapy for at least three months is necessary after surgery for valve replacement and valvuloplasty; therefore, treating the infectious disease was also important, although we were careful

**Table 2. Concomitant Warfarin and Linezolid Administration-induced Changes in Laboratory Test Values**

| | Before concomitant administration | During concomitant administration | At completion of concomitant administration | 1 week after completion |
|---|---|---|---|---|
| AST | 25.2±7.36 | 26.2±4.88 | 18.8±9.09 | 18.8±6.43 |
| ALT | 27.8±7.6 | 31.8±10.6 | 26.3±18.1 | 22.2±21.8 |
| BUN | 17.1±5.01 | 13.2±5.27 | 15.2±4.59 | 17.8±5.75 |
| Scr | 0.87±0.31 | 0.83±0.26 | 0.93±0.21 | 0.85±0.27 |
| Alb | 2.75±0.39 | 2.87±0.20 | 3.39±0.47 | 3.68±0.59 |

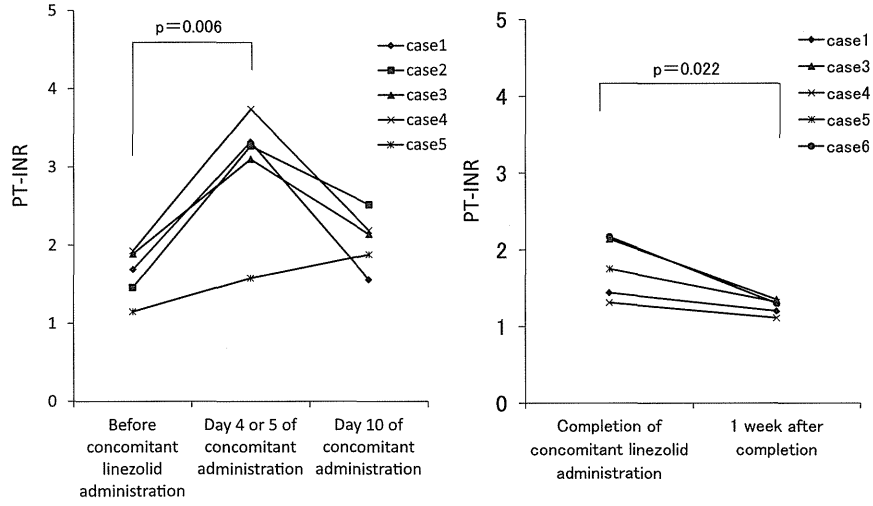


**Figure 1. Changes in the PT-INR values during and at the completion of concomitant warfarin and linezolid administration. The PT-INR values significantly increased from 1.62±0.32 before concomitant linezolid administration to 3.00±0.83 on day 4 or 5 of concomitant treatment ($p<0.01$) and decreased on day 10 due to dose reduction or the withdrawal of warfarin and the concomitant administration of rifampicin. The administration of warfarin was discontinued for surgery after the completion of the concomitant therapy and switched to vitamin K in one patient. Excluding this patient, the PT-INR values significantly decreased from 1.65±0.45 at the completion of treatment to 1.26±0.1 at one week after the completion of treatment ($p<0.05$).**

to monitor for a bleeding tendency in the four patients who required warfarin despite it being contraindicated in cases involving treatment for infectious endocarditis. Linezolid was started postoperatively in five cases. The mean duration of linezolid administration was 27.3±13.8 days, and the dose of linezolid was 600 mg IV every 12 hours in all patients. The infectious diseases improved following the administration of linezolid.

The liver and renal functions were in the normal range at the time of initiation of concomitant warfarin and linezolid therapy in all cases. The changes in the laboratory values, excluding PT-INR, are shown in Table 2. Consequently, concomitant warfarin and linezolid treatment did not induce significant changes in any of the following indicators: AST, ALT, BUN, Scr, BUN or Alb. In addition, no other concomitant drugs were administered before the maximum PT-INR was reached after the initiation of concomitant linezolid and warfarin in any of the patients, and no other concomitant drugs were administered one week after the completion of the concomitant therapy.

The changes in the PT-INR values are shown in Figs. 1 and 2. There were no significant changes in the PT-INR values three days before or on the day of initiation of concomitant treatment, and the dose of warfarin was not changed in any of the patients, with the exception of one case in which the warfarin dose was increased from 4 to 4.5 mg. In Case 6, treatment with linezolid was started with the administration of warfarin. Excluding this patient, the PT-INR values significantly increased from 1.62±0.32 before concomitant linezolid administration to 3.00±0.83 on day 4 or 5 of concomitant therapy ($p<0.01$) and then decreased by day 10 due to dose reduction or the withdrawal of warfarin and the concomitant administration of rifampicin. No bleeding tendency, as assessed according to the results of PT-INR monitoring, was observed in any of the patients, either after dose reduction or the withdrawal of warfarin following the concomitant administration of warfarin and linezolid. In Case 2, the administration of warfarin was discontinued for surgery after the completion of the concomitant therapy and the drug regimen was switched to vitamin K. Excluding this patient, the PT-INR values significantly decreased from 1.65±0.45 at completion to 1.26±0.1 at one week after completion ($p<0.05$).

Fig. 2 shows the relationship between the dose of war-